Solid State Phenomena Vol. 201 (2013) pp 131-158
Online available since 2013/May/14 at www.scientific.net

doi:10.4028/www.scientific.net/SSP.201.131

Applications of Nanostructured Materials as Gas Sensors

Ravi Chand Singh[1a], Manmeet Pal Singh[2b] and Hardev Singh Virk[3c]

[1]Department of Physics, Guru Nanak Dev University, Amritsar, India

[2]Department of Applied Sciences, Khalsa College of Engineering & Technology, Amritsar, India

[3]Department of Physics, Eternal University, Baru Sahib, HP, India

[a]ravichand.singh@gmail.com, [b]palmanmeet@gmail.com, [c]hardevsingh.virk@gmail.com

Keywords: Metal oxide Semiconductors, Gas Sensors, Surface energy, Grain size, Tin oxide, Sensor response, Sintering temperature.

Abstract. Gas detection instruments are increasingly needed for industrial health and safety, environmental monitoring, and process control. To meet this demand, considerable research into new sensors is underway, including efforts to enhance the performance of traditional devices, such as resistive metal oxide sensors, through nano-engineering. The resistance of semiconductors is affected by the gaseous ambient. The semiconducting metal oxides based gas sensors exploit this phenomenon. Physical chemistry of solid metal surfaces plays a dominant role in controlling the gas sensing characteristics. Metal oxide sensors have been utilized for several decades for low-cost detection of combustible and toxic gases. Recent advances in nanomaterials provide the opportunity to dramatically increase the response of these materials, as their performance is directly related to exposed surface volume. Proper control of grain size remains a key challenge for high sensor performance.

Nanoparticles of SnO_2 have been synthesized through chemical route at 5, 25 and 50^oC. The synthesized particles were sintered at 400, 600 and 800^oC and their structural and morphological analysis was carried out using X-ray diffraction (XRD) and transmission electron microscopy (TEM). The reaction temperature is found to be playing a critical role in controlling nanostructure sizes as well as agglomeration. It has been observed that particle synthesized at 5 and 50^oC are smaller and less agglomerated as compared to the particles prepared at 25^oC. The studies revealed that particle size and agglomeration increases with increase in sintering temperature. Thick films gas sensors were fabricated using synthesized tin dioxide powder and sensing response of all the sensors to ethanol vapors was investigated at different temperatures and concentrations. The investigations revealed that sensing response of SnO_2 nanoparticles is size dependent and smaller particles display higher sensitivity.

Table of Contents

1. Introduction

With ever increasing pollutants in our ambient, there is an urgent demand for reliable and cost effective sensors for monitoring them. These sensing devices are broadly classified into physically and chemically sensitive devices. Physically sensitive sensors measure various physical quantities such as pressure, temperature, velocity, acceleration, flow, liquid level, magnetic field etc. Chemical sensors measure concentration change of chemical species in liquid and gaseous media [1]. The chemically sensitive solid-state devices discussed in this article are based on the electrical response of the solid to its chemical environment. Hence solids like tin oxide (SnO_2) whose electrical properties are affected by the presence of a gas-phase or liquid-phase species have drawn attention of numerous researchers to fabricate prototype sensing devices. This change in electrical properties is observed and then used to detect chemical species.

The major advantages of solid-state sensors are that they are very simple to operate, small in size and low cost of construction. The major disadvantages of most solid-state chemical sensors are lack of stability, reproducibility, and selectivity.

The term solid-state sensors has been broadly used to classify the sensors based upon classical semiconductors, solid electrolytes, insulators, metals and catalytic materials including different types of organic membranes. Over the past few decades solid state gas sensors based on metal oxides have become the predominant solid-state devices for gas alarms used in domestic, commercial and industrial premises. Large variety of ceramic thick-film and thin film devices has been developed over the years with mostly an empirical optimization of their performance [1, 2]. Numerous materials have been reported to be important and usable as metal oxide sensors including both single- (e.g., ZnO, SnO_2, WO_3, TiO_2, and Fe_2O_3) and multi-component oxides ($BiFeO_3$, $MgAl_2O_4$, $SrTiO_3$, and $Sr_{1-y}Ca_yFeO_{3-x}$) [3-5]. The mechanism for gas detection in these materials is based, in large part, on reactions that occur at the sensor surface, resulting in a change in the concentration of adsorbed oxygen. Oxygen ions adsorb onto the material's surface, removing electrons from the bulk and creating a potential barrier that limits electron movement and conductivity. When reactive gases of reducing nature combine with this oxygen, the height of the barrier is reduced, increasing conductivity. This change in conductivity is directly related to the amount of a specific gas present in the environment, resulting in a quantitative determination of gas presence and concentration.
Resistive metal oxide sensors comprise a significant part of the gas sensor component market, which generated revenues of approximately $1.5B worldwide in 1998. Significant growth is projected, and the market should exceed $2.5B by 2010. While many different approaches to gas detection are available, metal oxide sensors remain a widely used choice for a range of gas species. These devices offer low cost and relative simplicity, advantages that should work in their favor as new applications emerge [6].

It has been established that the materials in different structural states can be used in resistive type gas sensors. These states include amorphous-like state, glass-state, nanocrystalline state, polycrystalline state and single crystalline state. Each state has its own unique properties and characteristics that can affect sensor performance. However, in practice nanocrystalline and polycrystalline materials have found the greatest application in solid state gas sensors [7-12]. Nanocrystalline and polycrystalline materials have the optimal combination of critical properties for sensor application including high surface area due to small crystallite size, cheap design technology and stability of both structural and electro-physical properties.

Nano- and polycrystalline materials are very complicated objects for study, because the electro-conductivity of these materials depends on a number of factors [4, 13-16]. It is necessary to understand the role of morphology and crystallographic structure in gas sensing effects. A number of authors have tried to establish the relation between structural parameters and sensing response. However, one cannot find large number of good works in this context. Yamazoe and co-workers [13, 17, 18] have tried to find the correlation between grain size of metal oxides and response of gas sensors. Egashira and co-workers [19-21] studied the influence of porosity of the material on the sensing response. Cabo et al. [22] and Cirera et al. [23] studied the dependence of sensing response on the structural properties of metal oxide.

Several recent research reports have confirmed the benefits of nanoengineering on sensor performance [6]. Rella et al. [24] demonstrated good response to NO_2 and CO when the SnO_2 grain size was controlled below 10 nm. Ferroni et al. [25] demonstrated good response to NO_2 for solid solutions of TiO_2 and WO_3 when grain size was held at near 60 nm. Chung et al. [26] demonstrated that increasing the firing temperature (which increases grain size) significantly reduces the response of WO_3 sensors to NO_x. Chiorino et al. [27] also demonstrated that firing temperature plays a key role in the response of SnO_2 sensors, with films treated to 650°C showing nearly twice the response to NO_2 as films treated at 850°C.

In this review paper, it has been attempted to correlate the role of nanostructured materials as the potential candidates for the gas sensing phenomenon. Before studying the effect of structural parameters on gas sensing characteristics, it is of utmost importance to explain the basis of sensing principle briefly, and surface chemistry of nanomaterials.

2. Principle of Gas Sensing by Metal Oxide Semiconductors

It has been a well known fact that the resistance of semiconductors is affected by the gaseous ambient. The semiconducting metal oxides based gas sensors exploit this phenomenon. Semiconductor material's sensing mechanism can be understood as the reaction between semiconductor surface and gases in the atmosphere, which changes the conductance of semiconductor. This change in the conductivity of the semiconductor in the gaseous ambient may be attributed to the adsorption mechanism: Oxygen from the atmosphere adsorbs and extracts electrons from the semiconductor. If electrons dominate the conduction mechanism in the solid, then conductivity will decrease as the electrons are extracted. When an organic vapour, or any reducing gas, is present in the atmosphere, it reacts with the negatively charged oxygen, becoming oxidized and the electrons are returned to the solid, restoring the conductivity. Other possible reason for this resistance change can be the reaction between the semiconductor and the gas, resulting in the ion exchange near the surface.

Another reason that can satisfactorily explain the change in the conductance of semiconductor is that the reaction between gas and semiconductor may lead to the change in the stoichiometry or due to formation of another compound. This may be interpreted as if lattice oxygen is extracted when some organic vapours are introduced into the atmosphere. Therefore, the presence of the organic vapour lowers the cation/oxygen ratio in the semiconductor oxide, that is how it changes the stoichiometry of the solid. Such a change in the stoichiometry can have significant effect on the conductivity of the material.

First commercial sensor designed out of semiconducting metal oxide was based on the SnO_2 because tin oxide is chemically inert and it was used in the compressed powder form to detect the reducing gases. The most attractive feature of these types of sensors is that they are low cost. But the problem of reproducibility exists in these types of sensors due to its dependence on the inter-granular resistance, a parameter varying with small details of the preparation; each sensor can be

expected to differ slightly in its initial characteristics. As the sensor operates at high temperature, slow drift due to stoichiometry changes or irreversible reactions with gaseous impurities in the atmosphere affect its stability. Sensing response depends upon the catalysis. Selectivity is another bottleneck which has to be sort out, and intensive investigations are going around the world to develop the device which will be free of all the above mentioned problems. The operation of semiconductor gas sensor is very complex, so undoubtedly the progress is slow and each step in this direction will open a new avenue for these low-cost sensors.

3. Nanocrystalline Materials

Nanotechnology deals with small structures or small-sized materials. The typical dimension spans from sub-nanometer to several hundred nanometers. A nanometer (nm) is one billionth of a meter, or 10^{-9} m. One nanometer is approximately the length equivalent to 10 hydrogen or 5 silicon atoms aligned in a line. Small features permit more functionality in a given space, but nanotechnology is not just a simple continuation of miniaturization from micron meter scale down to nanometer scale. Materials in the micrometer scale mostly exhibit physical properties the same as that of bulk form; however, materials in the nanometer scale may exhibit physical properties distinctively different from that of bulk. Materials in this size range exhibit some remarkable specific properties; a transition from atoms or molecules to bulk form takes place in this size range. For example, crystals in the nanometer have a low melting point (the difference can be as large as 1000°C) and reduced lattice constants, since the number of surface atoms or ions becomes a significant fraction of the total number of atoms or ions and the surface energy plays a significant role in the thermal stability. Crystal structures unstable at elevated temperatures are stable at much lower temperatures in nanometer sizes, so ferroelectrics and ferromagnetics may lose their ferroelectricity and ferromagnetism when the materials are shrunk to the nanometer scale. Bulk semiconductors become insulators when the characteristic dimension is sufficiently small (in a couple of nanometers). Although bulk gold does not exhibit catalytic properties, gold nanocrystal demonstrates to be an excellent low temperature catalyst.

In order to explore novel physical properties and phenomena and realize potential applications of nanostructures and nanomaterials, the ability to fabricate and process nanomaterials and nanostructures is the first corner stone in nanotechnology. Nanostructured materials are those with at least one dimension falling in nanometer scale, and include nanoparticles (including quantum dots, when exhibiting quantum effects), nanorods and nanowires, thin films, and bulk materials made of nanoscale building blocks or consisting of nanoscale structures. Many technologies have been explored to fabricate nanostructures and nanomaterials. These technical approaches can be grouped in several ways. One way is to group them according to the growth process:

(1) Vapor phase growth, including laser reaction pyrolysis for nanoparticles synthesis and atomic layer deposition (ALD) for thin film deposition.

(2) Liquid phase growth, including colloidal processing for the formation of nanoparticles and self assembly of mono-layers.

(3) Solid phase formation, including phase segregation to make metallic particles in glass matrix and two-photon induced polymerization for the fabrication of three-dimensional photonic crystals.

(4) Hybrid growth, including vapor-liquid-solid (VLS) growth of nanowires.

Another way is to group the techniques according to the form of products:

(1) Nanoparticles by means of colloidal processing, flame combustion and phase segregation.

(2) Nanorods or nanowires by template-based electroplating, solution liquid- solid growth (SLS), and spontaneous anisotropic growth.

(3) Thin films by molecular beam epitaxy (MBE) and atomic layer deposition (ALD).

(4) Nanostructured bulk materials, for example, photonic band gap crystals by self-assembly of nanosized particles.

There are many other ways to group different fabrication and processing techniques such as top-down and bottom-up approaches, spontaneous and forced processes. Top-down is in general an extension of lithography. The concept and practice of a bottom-up approach in material science and chemistry are not new either. Synthesis of large polymer molecules is a typical bottom-up approach, in which individual building blocks (monomers) are assembled to a large molecule or polymerized into bulk material. Crystal growth is another bottom-up approach, where growth species either atoms, or ions or molecules orderly assemble into desired crystal structure on the growth surface.

3.1 Bottom-Up and Top-Down Approaches. Obviously there are two approaches to the synthesis of nanomaterials and the fabrication of nanostructures: top-down and bottom-up. Attrition or milling is a typical top-down method in making nanoparticles, whereas the colloidal dispersion is a good example of bottom-up approach in the synthesis of nanoparticles. Lithography may be considered as a hybrid approach, since the growth of thin films is bottom-up whereas etching is top-down, while nanolithography and nanomanipulation are commonly a bottom-up approach. Both approaches play very important roles in modern industry and most likely in nanotechnology as well. There are advantages and disadvantages in both approaches.

Among others, the biggest problem with top-down approach is the imperfection of the surface structure. It is well known that the conventional top-down techniques such as lithography can cause significant crystallographic damage to the processed patterns, and additional defects may be introduced even during the etching steps. For example, nanowires made by lithography are not smooth and may contain a lot of impurities and structural defects on surface. Such imperfections would have a significant impact on physical properties and surface chemistry of nanostructures and nanomaterials, since the surface over volume ratio in nanostructures and nanomaterials is very large. The surface imperfection would result in a reduced conductivity due to inelastic surface scattering, which in turn would lead to the generation of excessive heat and thus impose extra challenges to the device design and fabrication. Regardless of the surface imperfections and other defects that top-down approaches may introduce, they will continue to play an important role in the synthesis and fabrication of nanostructures and nanomaterials.

Bottom-up approach is often emphasized in nanotechnology literature, though bottom-up is nothing new in materials synthesis. Typical material synthesis is to build atom by atom on a very large scale, and has been in industrial use for over a century. Examples include the production of salt and nitrate in chemical industry, the growth of single crystals and deposition of films in electronic industry. For most materials, there is no difference in physical properties of materials regardless of the synthesis routes, provided that chemical composition, crystallinity, and microstructure of the material in question are identical. Of course, different synthesis and processing approaches often result in appreciable differences in chemical composition, crystallinity, and microstructure of the material due to kinetic reasons. Consequently, the material exhibits different physical properties. Bottom-up approach refers to the build-up of a material from the bottom: atom-by-atom, molecule-by-molecule, or cluster-by-cluster. In organic chemistry and/or polymer science, we know polymers are synthesized by connecting individual monomers together. In crystal growth, growth species, such as atoms, ions and molecules, after impinging onto the growth surface, assemble into crystal structure one after another. Although the bottom-up approach is nothing new, it plays an important role in the fabrication and processing of nanostructures and nanomaterials. There are several reasons for this. When structures fall into a nanometer scale, there is little choice for a top-down approach. All the tools we have possessed are too big to deal with such tiny subjects.

Bottom-up approach also promises a better chance to obtain nanostructures with less defects, more homogeneous chemical composition, and better short and long range ordering. This is because the bottom-up approach is driven mainly by the reduction of Gibbs free energy, so that nanostructures and nanomaterials thus produced are in a state closer to a thermodynamic equilibrium state. On the contrary, top-down approach most likely introduces internal stress, in addition to surface defects and contaminations.

4. Physical Chemistry of Solid Surfaces

Nanostructures and nanomaterials possess a large fraction of surface atoms per unit volume. The ratio of surface atoms to interior atoms changes dramatically if one successively divides a macroscopic object into smaller parts. This dramatic increase in the ratio of surface atoms to interior atoms in nanostructures and nanomaterials might illustrate why changes in the size range of nanometers are expected to lead to great changes in the physical and chemical properties of the materials. The total surface energy increases with the overall surface area, which is in turn strongly dependent on the dimension of material. Due to the vast surface area, all nanostructured materials possess a huge surface energy and, thus, are thermodynamically unstable or metastable. One of the great challenges in fabrication and processing of nanomaterials is to overcome the surface energy, and to prevent the nanostructures or nanomaterials from growth in size, driven by the reduction of overall surface energy. In order to produce and stabilize nanostructures and nanomaterials, it is essential to have a good understanding of surface energy of solid surfaces.

4.1 Surface Energy. Atoms or molecules on a solid surface possess fewer nearest neighbors or coordination numbers, and thus have dangling or unsatisfied bonds exposed to the surface. Because of the dangling bonds on the surface, surface atoms or molecules are under an inwardly directed force and the bond distance between the surface atoms or molecules and the sub-surface atoms or molecules, is smaller than that between interior atoms or molecules. When solid particles are very small, such a decrease in bond length between the surface atoms and interior atoms becomes significant and the lattice constants of the entire solid particles show an appreciable reduction. The extra energy possessed by the surface atoms is described as surface energy, surface free energy or surface tension. Surface energy, γ, by definition, is the energy required to create a unit area of "new" surface:

$$\gamma = \left(\frac{\partial G}{\partial A} \right)_{n_i\, T, P} \tag{4.1}$$

where A is the surface area. Let us consider separating a rectangular solid material into two pieces as illustrated in Fig. 1. On the newly created surfaces, each atom is located in an asymmetric environment and will move towards the interior due to breaking of bonds at the surface. An extra force is required to pull the surface atoms back to its original position. Such a surface is ideal and also called singular surface. For each atom on such a singular surface, the energy required to get it back to its original position will be equal to the number of broken bonds, N_b, multiplying by half of the bond strength, ε. Therefore, the surface energy is given by:

$$\gamma = \frac{1}{2} N_b \varepsilon \rho_a \tag{4.2}$$

where ρ_a is the surface atomic density, the number of atoms per unit area on the new surface.

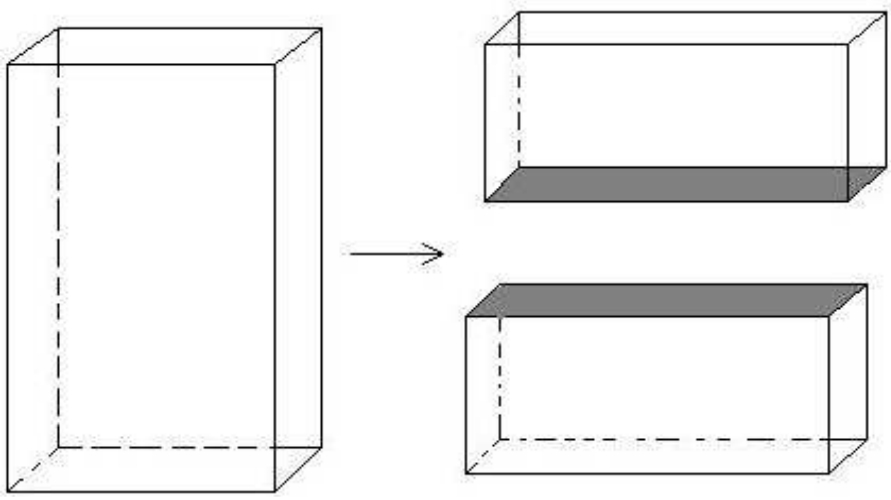

Fig. 1 Schematic showing two new surfaces being created by breaking a rectangular solid into two pieces

This relation only gives a rough estimation of the true surface energy of a solid surface, and is only applicable to solids with rigid structure where no surface relaxation occurs. When there is an appreciable surface relaxation, such as the surface atoms moving inwardly, or there is a surface restructuring, surface energy will be lower than that estimated by the above equation.

Thermodynamics tells us that any material or system is stable only when it is in a state with the lowest Gibbs free energy. Therefore, there is a strong tendency for a solid or a liquid to minimize the total surface energy. There are a number of mechanisms to reduce the overall surface energy. The various mechanisms can be grouped into atomic or surface level, individual structures and the overall system.

For a given surface with a fixed surface area, the surface energy can be reduced through (i) surface relaxation, the surface atoms or ions shift inwardly which occur more readily in liquid phase than in solid surface due to rigid structure in solids, (ii) surface restructuring through combining surface dangling bonds into strained new chemical bonds, (iii) surface adsorption through chemical or physical adsorption of terminal chemical species onto the surface by forming chemical bonds or weak attraction forces such as electrostatic or van der Waals forces, and (iv) composition segregation or impurity enrichment on the surface through solid-state diffusion.
At the overall system level, mechanisms for the reduction of overall surface energy include (i) combining individual nanostructures together to form large structures so as to reduce the overall surface area, if large enough activation is available for such a process to proceed, and (ii) agglomeration of individual nanostructures without altering the individual nanostructures. Specific mechanisms of combining individual nanostructures into large structures include (a) sintering, in which individual structures merge together, and (b) Ostwald ripening, in which relatively large structures grow at the expense of smaller ones. In general, sintering is negligible at low temperatures including room temperature, and becomes important only when materials are heated to elevated temperatures, typically 70% of the melting point of the material. Ostwald ripening occurs at a wide range of temperatures and proceeds at relatively low temperatures when nanostructures are dispersed and have an appreciable solubility in a solvent.

5. Structural Parameters of Metal Oxides Controlling Gas-sensing Characteristics

As discussed earlier that the sensor operation is based upon the change in the resistance (or conductance) of the gas-sensing material induced by the surrounding gas. The changes are caused by the various processes which take place both at the surface and in the bulk of gas-sensing material

[9, 11, 14, 28, 29]. Fig. 2 represents the possible parameters which control the gas sensing properties pictorially.

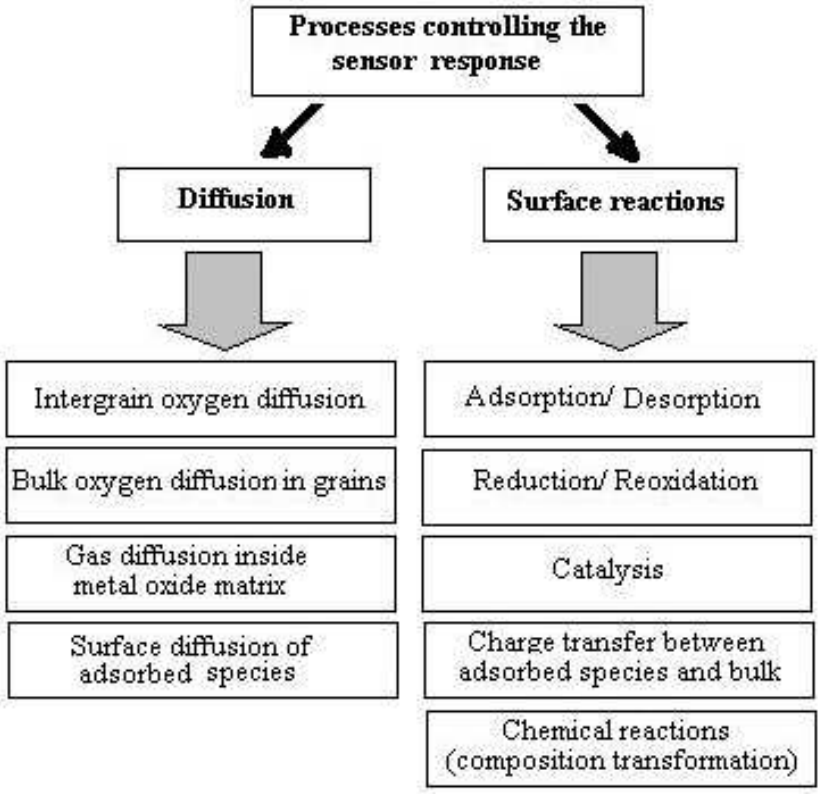

Fig. 2 Pictorial diagram illustrating the processes controlling the sensor response

Research has confirmed that all the processes indicated in Fig. 2 including adsorption/ desorption, catalysis, reduction/ reoxidation, and diffusion are relevant in gas sensors and influenced by structural parameters of the sensor material. As gas sensing is a complex mechanism and it depends on numerous factors, it is clear that we have to consider the influence of a number of structural parameters of metal oxide matrix on gas sensors response. These parameters are enumerated as thickness, grain size, porosity, grain faceting, agglomeration, film texture, surface geometry, sensor geometry, surface disordering, bulk stoichiometry, grain network, active surface area and size of necks.

5.1Grain Size Influence on Gas-sensing. Proper control of grain size remains a key challenge for high sensor performance [6]. The thick film devices must be heated to sufficiently high temperatures to ensure interconnectivity between individual grains and film robustness. However, if the processing temperature is too high, substantial grain growth can occur, coupled with a rapid decrease in open porosity, resulting in a marked decrease in sensor response.

Work has been carried out to study the effect of microstructure on the electro-physical properties of the polycrystalline materials; moreover, acceptable models based on grains and necks have been formulated to rationalize the phenomenon [9, 13, 30, 31]. It has been established that the grain size and the width of the necks are the main parameters that control gas-sensing properties in metal oxide films as well. It has been tried to evaluate the impact of grains size and necks size on the sensor response in the frame of modern gas sensor models [9, 13, 30, 31]. Usually, it is explained through so-called “dimension effect”, a comparison of the grains size (d) or neck width (x) with the Debye length (L_D)

$$L_D = \sqrt{\frac{\varepsilon kT}{2\pi e^2 N}} \tag{5.1}$$

where k is Boltzmann constant, T is the absolute temperature, ε is the dielectric constant of the material and N is the concentration of charge carriers.

In brief, for explanation of the "dimension effect" on the gas-sensing effect, it is possible to provide the following argument as reported in the literature [30, 32]. For large crystallites with grain diameter, $d >> 2L_s$, where L_s is the width of surface space charge ($L_s = L_D\sqrt{eV_s^2 / kT}$), and for a small width of necks ($d < L_s$), the conductance of both the film and ceramics usually is limited by Schottky barriers (V_s) at the grain boundary. In this case, the sensitivity is practically independent of d.

In the case of $d \sim 2L_s$, every conducting channel in necks between grains is overlapped. If the number of long necks is much larger than the inter-grain contacts, they control the conductivity of the gas-sensing material and define the size dependence of the gas sensitivity.

If $d < 2L_s$, every grain is fully involved in space-charge layer and the electron transport is affected by the charge at the adsorbed species. It has been demonstrated that when the grain size becomes comparable to twice the Debye length, a space-charge region can develop in the whole crystallite [33]. The latter case is the most desirable, since it allows achievement of maximum sensor response.

Yamazoe [17] has given a simple model analysis for SnO_2 crystallites where grain boundary control, neck control and grain control are represented schematically in figure 3. The neck size (X) was found to
be roughly proportional to the crystallite grain size (D), being well approximated by X = 0.8D with a maximum deviation of nearly 10% for both pure SnO_2 samples and stabilized samples. It was also revealed that each crystallite was coordinated with four neighbours on average by necks. For simplicity, the sensor element is presented by a one-dimensional chain of SnO_2 crystallites which are connected by a predominant number of necks and a small number of grain boundary contacts. For D >> 2L, the electron conducting channels through necks are too wide to be influenced by the surface effect. The grain-boundary contacts share most of the electrical resistance of the chain so that they govern the gas sensitivity (grain boundary control). This can explain why the gas sensitivity is almost independent of D in this region. When D decreases to come closer to 2L, the necks become the most resistive part in the chain and thus control the gas sensitivity (neck control). Finally, when D < 2L, each constituent grain is depleted of conduction electrons as a whole. Under this situation, grains share a major part of the resistance of the chain and control the gas sensitivity (grain control).

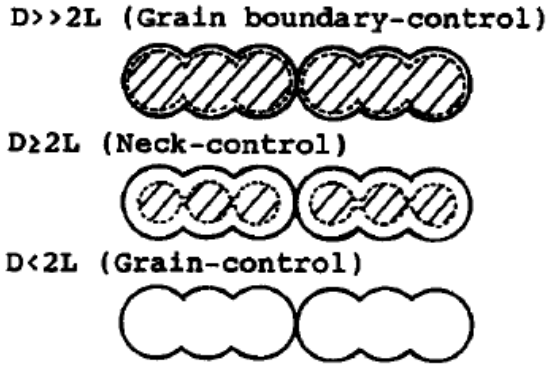

Fig. 3 Schematic models for the grain-size effects. Hatched part shows core region (low resistivity), while unhatched shows the space-charge region (high resistivity) [17]

Yamazoe [17] has suggested that it is necessary to note that the applicability of "grains" or "necks" models depends strongly on the technological routes used for metal oxides synthesis or deposition and sintering conditions. Usually the appearance of necks is a result of high temperature annealing (T_{an} > 700-800^{o}C). Taking into account processes which take place at inter-grain interfaces during high temperature annealing, one can assume that the forming of long necks in inter-grain space is a consequence of mass transport from one grain to another. According to Xu et al. [13], for metal oxide samples after high temperature annealing, the neck size (X) is proportional to grain size (d) with proportionality constant (X/d) of 0.8 ± 0.1. However, it is necessary to note that this constant depends on the sintering parameters. For thin metal oxide film and ceramics, which were not subjected to high temperature treatments, the gas-sensing matrix is formed from separately grown grains. Therefore, in such metal oxides, the necks between grains are very short or are absent. It means that for description of their gas sensing properties we can use the "grains" model. According to this model, between the grains there are Schottky type contacts with the height of potential barrier depending on the surrounding atmosphere. In the frame of such approach, the grain boundary space charge or band bending on inter-grain interfaces are the main parameters controlling the conductivity of nanocrystalline metal oxides.

It has been studied that SnO_2 films with grain size equating 5-14 nm, and at low operating temperatures (25-300^{o}C), both the grain and grain boundary contribute to the conductivity [34]. At higher operating temperatures (above 300^{o}C), the grain boundary contribution for the conductivity is dominant. The impedance of these films was mainly contributed by the potential barriers at grain boundaries.

Experimentally, it has been confirmed that the grain size influences the sensor response and drastic increase was observed in sensitivity for SnO_2 based gas sensor with grain size smaller than a Debye length [13, 35, 36]. The sensitivity of sensors based on tin oxide nanoparticles dramatically increased when the particle size was reduced down to 6 nm. Below this critical grain size, sensor sensitivity rapidly decreased [37]. Debye length of SnO_2 was calculated to be L_D = 3 nm at 250 ^{o}C, the highest sensitivity was actually reached when the particle diameter corresponded to 2 nm [33]. Grain size effects were considered, in particular, in semiconductor gas sensors, which contained mixture of necks and grain boundary contacts, and concluded that the gas sensitivity would increase sharply for particle diameter below about 35 nm [38]. The devices fabricated out of SnO_2 particles of 20 nm were around 10 times more sensitive than the sensors fabricated from 25 to 45 nm particles [39].

Because the Debye length depends on the concentration of free charge carriers (Eqn. 5.1), it becomes clear that the observed variation of threshold value of crystallite's size is valid. Moreover, this parameter must be dependent on the material's properties and doping. It has been observed that the decrease of free charge carriers concentration, through stoichiometry improvement induced by annealing or doping, can considerably increase this threshold value [13].

Besides, the surface reactivity of particles is known to rapidly increase with the increase of the surface-to-bulk ratio, because the strong curvature of the particle surface generates a larger density of defects, which are the most reactive surface sites. This high reactivity has largely been taken advantage in catalysis, where ultrafine particles have been used for decades. It was found that when properly processed during the fabrication of chemical semiconductor sensors, these nanoparticles are sufficiently reactive to make the use of catalytic additives redundant and to decrease the working temperature of the sensors without any loss of sensitivity [40, 41].

However, the decrease in grain size cannot be unlimited. At some critical dimension, the number of free electrons in the grain could become zero even at V_s = 0. This leads to grain resistance that would not be dependant on the changes in the surrounding atmosphere. For charge carrier

concentration in metal oxides of 10^{-21} cm^{-3}, the critical crystallite size is 1 nm. It was reported that the use of finely dispersed small crystallites can also have a deleterious effect on temporal stability of the sensor [36]. Rao et al. [42] have shown that an excessive decrease of grain size leads to a loss of structural stability, and as a consequence, to change of both surface and catalytic properties of the material. It was found that SnO_2 with grain size of 1-4 nm, grain growth process begins at temperatures ~ 200-400 ^oC. In contrast, SnO_2 crystallites, with average sizes ranging from 1.7-4.0 μm, were stable up to 1050 ^oC [43].

There are two main reasons for grain growth during thermal treatments [34, 45]. This instability may arise from a known defect in the bulk state, such as faulty stoichiometry, or due to the finite size of the grains. A quantum mechanical study of the stability of SnO_2 nanocrystalline grains has shown that the increase of both the grain size in the range 0.3-4.0 nm, and the oxygen content in SnO_2 increased the stability of SnO_2 grains. A well known fact is that the size has a strong influence on the melting temperature; the decrease of the grain size is accompanied by lowering of the melting temperature of the semiconductor nanocrystals as well [46-48].

The principle of surface and interface energy minimization explains only the appearance of a driving force for the recrystallization of polycrystalline films during the annealing. The principle cannot account for the threshold nature of the grain size changes, i.e., the presence of a threshold temperature (T_{st}) below which the crystallites with the fixed size remain stable, and the absence of $t^{1/2}$ type grain size dependence on time during thermal annealing.

It thus becomes clear that the presence of a finely dispersed fraction with a grain size smaller than 2-5 nm will lead to some structural instability of the metal oxide matrix at moderate operating temperatures ($T < 600^oC$). This is true even for films with average grain sizes greater than 100 nm. Therefore, future design methods of nano-scale devices, which assure grain size stabilization during long term operation at high temperature, will gain priority over the design of methods producing nano-scaled materials with minimal grain size. Synthesis of metal oxide powder and deposition of thin films with a small dispersion of grain size is an effective method for improvement of temporal stability of solid-state gas sensors. The grain sizes in thin films during the annealing process changes considerably less than in thick films. Therefore, unless there is a dire need to improve detection limits, it is not advisable to design sensors with excessively reduced grain sizes. This problem is utterly serious for operation in ambience of reducing gases.

6. Experimental Investigations of SnO_2 Nanostructures

Among commercial gas sensors, SnO_2 sensors have played a dominant role due to their high sensitivity, quick response, resistance to corrosion, etc. [49-51]. The reduction in particle size is one of the methods to improve the sensitivity of polycrystalline material based sensors [13, 52]. SnO_2 nanostructure based sensors have given a new dimension to investigations and these devices show excellent sensing properties [53-56].

Nanoparticles of SnO_2 can be produced by using a variety of techniques. The most common among these include sol-gel [57], spray pyrolysis [58], solvothermal [59] and microwave methods [60]. In the present work we have employed chemical method to synthesize nanoparticles. Although the technique is simple and inexpensive, yet the nanostructure morphology can be modified by varying reaction conditions to achieve the desired final product. One of the aims of the present study is to control the size of SnO_2 particles by changing the reaction temperature.

A high surface energy is associated with nanostructures. The system tends to reduce overall surface energy. This can be achieved either by combining individual nanostructures together to form large structures so as to reduce the overall surface area or by agglomeration of individual nanostructures

without altering the individual nanostructures. Sintering and Ostwald ripening are the specific mechanisms which combine individual nanostructures into large structures. Ostwald ripening, where large particles grow at the expense of smaller ones, proceeds in solution during synthesis provided enough aging time is given. We tried to lower Ostwald ripening by minimizing the aging after reaction. The sintering was the main process which altered the morphology of nanostructures in the present study. Sintering is the consolidation of a powder by means of prolonged use of elevated temperatures, which are, however, below the melting point of any major phase of the material. It facilitates the movement of atoms or molecules through the mechanism of mass transport that may be lattice diffusion, surface diffusion or evaporation-condensation and results in the grain growth which has detrimental effect on the properties of the material. The investigation of effect of sintering temperature on morphology and size of synthesized nanoparticles has been carried out in the present study.

The thin or thick film of active gas sensing material is deposited using a number of sophisticated techniques such as sputtering, screen printing, etc. [61-64]. However, thick film gas sensors based upon semiconductor oxides have certain advantages over other type of gas sensors, such as low cost, simple construction, small size and good sensing properties [65]. In the present study we have used thick slurry of tin oxide powder to deposit a thick film. Finally the sensing response of SnO_2 nanoparticles based sensor as function of temperature, particle size and concentration of ethanol has been studied.

6.1 Preparation of Tin dioxide Powder. Nanoparticles of tin dioxide powder were prepared through fine crystallization in liquid phase. The detailed preparation procedure is as follows: Ammonia water at 25^{o}C (room temperature) was added slowly to the 0.2 M solution of $SnCl_4$ and precipitate of tin hydroxide was produced. The material produced was separated from rest of the liquid by filtering, followed by drying at 120^{o}C. To investigate the effect of heat treatment on the morphology and sensing characteristics of tin dioxide powder, the material produced was divided into three parts and each part was sintered for three hours in air at 400, 600 and 800^{o}C, respectively.

In the present study, we wanted to devise some method to control the particle size by simple technique. To carry forward this idea in other experiments, the reactions during crystallization in liquid phase were carried out at 5^{o}C and 50^{o}C instead of room temperature. The powder synthesized at these temperatures was also divided into three parts and subjected to similar sintering procedure as mentioned for the first experiment. In this way, nine different samples of SnO_2 powder produced by different procedures were obtained.

6.2 Sensor Fabrication and its Testing. The synthesized SnO_2 powders were processed into water based pastes. The paste was coated onto an alumina substrate (12 mm x 5mm size) between gold electrical contacts (2mm apart) to obtain a thick film (~2μm thickness). These samples were heated at 350^{o}C for 30 minutes to give them final shape ready for sensing.

The sensing characteristics of SnO_2 sensors were obtained with a home built apparatus (Fig. 4a) consisting of a simple potentiometric arrangement and a test chamber of known volume in which a sample holder, a small temperature controlled oven and a mixing fan were installed. The fabricated sensor was placed in the oven kept at suitable temperature and a measured quantity of ethanol was injected into the test chamber. The variation of voltage signal across a resistance connected in series with sensor was monitored and recorded with a computer controlled data handling system (Fig. 4b). Same procedure was repeated for ethanol sensing with all the samples at temperatures varying from 200 to 400^{o}C. Ethanol vapour sensitivity (response magnitude) of the sensor was determined as the (G-Go)/Go ratio, where Go is the conductance of thick film sensor in an air ambience and G is the conductance in a mixture of air and ethanol vapours.

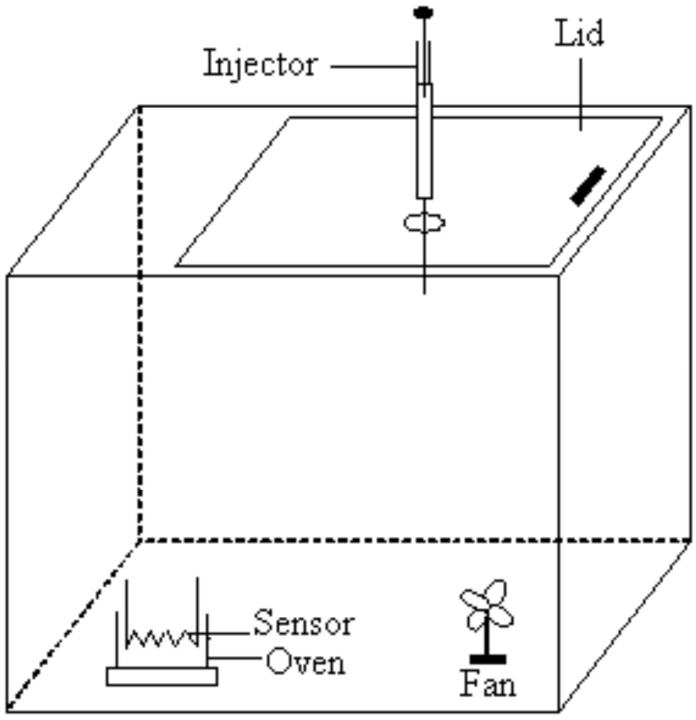

Fig. 4(a) Schematics of gas sensor testing chamber

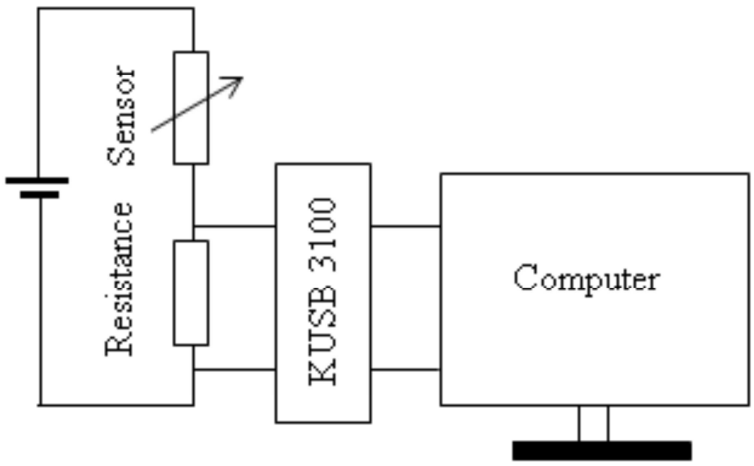

Fig. 4(b) Schematics of data acquisition system

6.3 Structural Analysis. Plots of X-ray diffraction data of tin dioxide samples prepared at 5^{o}C and sintered at 400, 600 and 800^{o}C, respectively, are shown in figure 5. The XRD plots of powder samples prepared at 25^{o}C and sintered at 400, 600 and 800^{o}C, respectively, are shown in figure 6. Similarly, figure 7 represents diffraction peaks of materials synthesized at 50^{o}C and sintered at 400, 600 and 800^{o}C, respectively. The diffraction pattern in all the plots are in agreement with the standard X-Ray diffraction peaks (JCPDS file 770451), which confirmed that the synthesized materials were SnO_2 of the tetragonal geometry.

The crystallite size 'D' was estimated from the peak width with Scherrer's formula, $D = K\lambda / \beta\cos\theta$, where λ is the X-ray wavelength, β is the full width at half maximum (FWHM) of a diffraction peak, θ is the diffraction angle, and K is the Scherrer's constant. The calculated sizes confirmed the particle growth with sintering temperature (Table 1).

Table 1 Comparison between sensitivity and particle size of SnO_2 at different synthesis parameters

Reaction Temperature (°C)	Sintering Temperature (°C)	Average Particle Size (nm)	Optimum Operating Temperature (°C)	% Sensitivity (200 ppm ethanol)
05	400 600 800	~02 ~24 ~28	250 250 300	1529 633 580
25	400 600 800	~10 ~15 ~ 40	350 350 350	1150 850 300
50	400 600 800	~05 ~20 ~32	250 300 300	1400 734 550

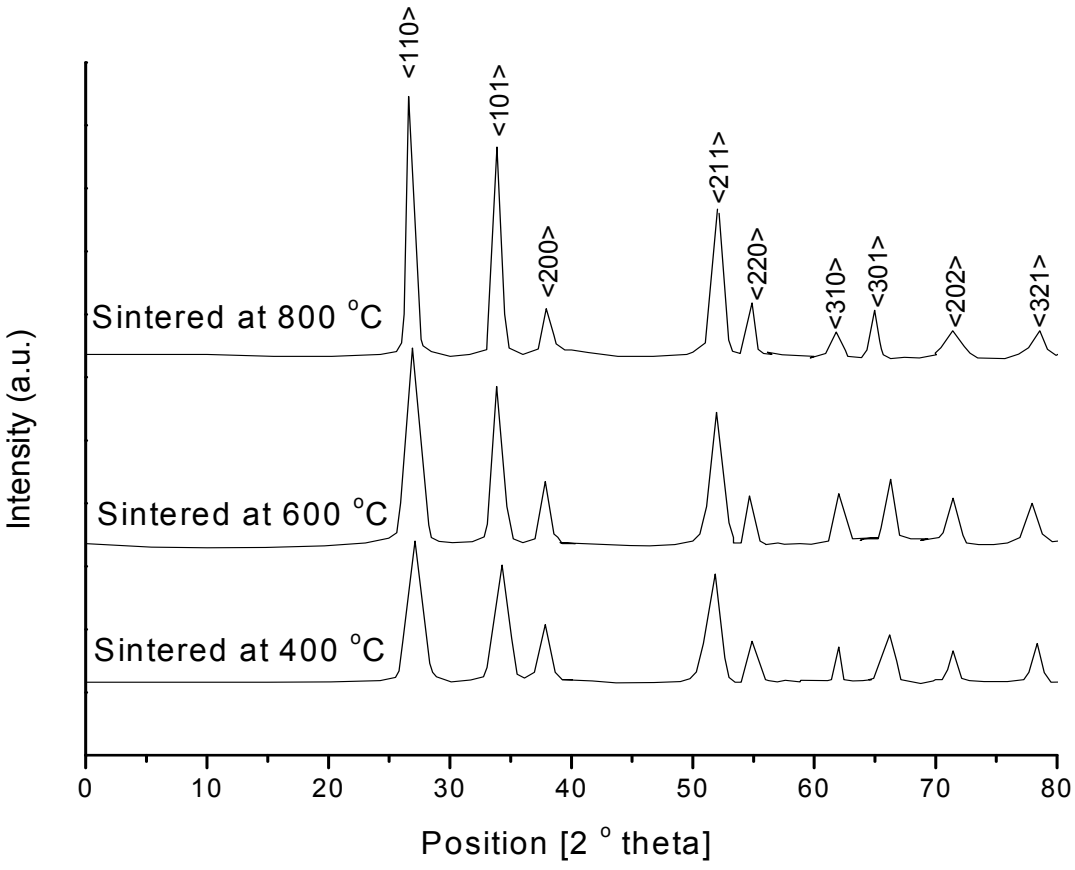

Fig. 5 XRD of SnO_2 powder synthesized at 5°C and sintered at 400, 600 & 800°C

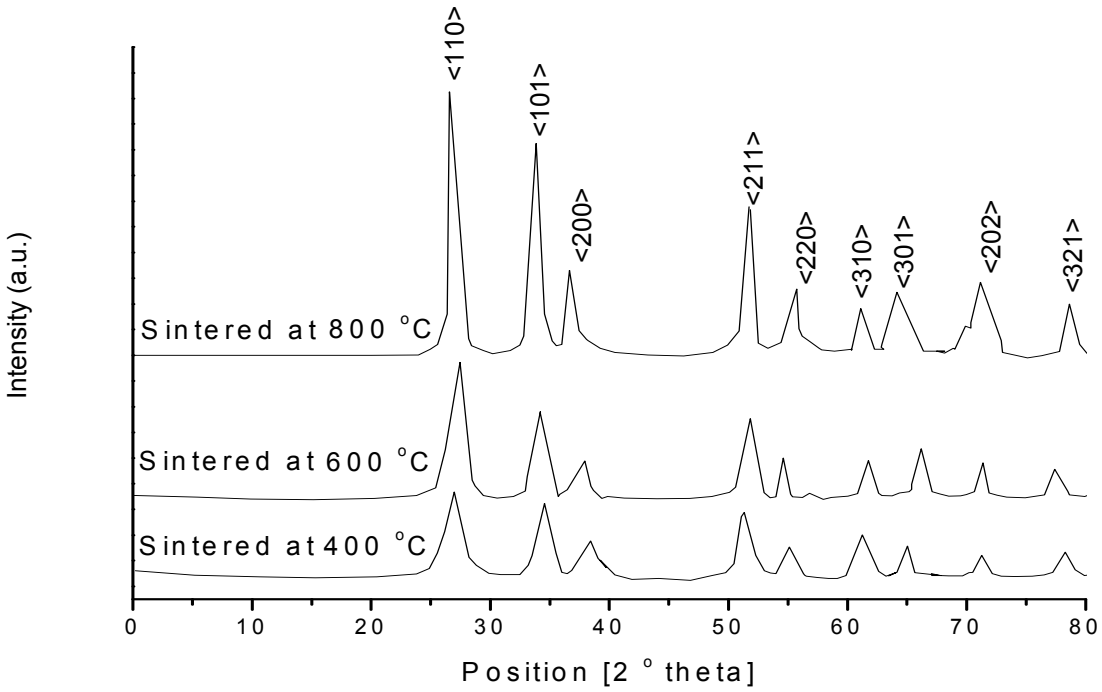

Fig. 6 XRD of SnO_2 powder synthesized at 25°C and sintered at 400, 600 & 800°C

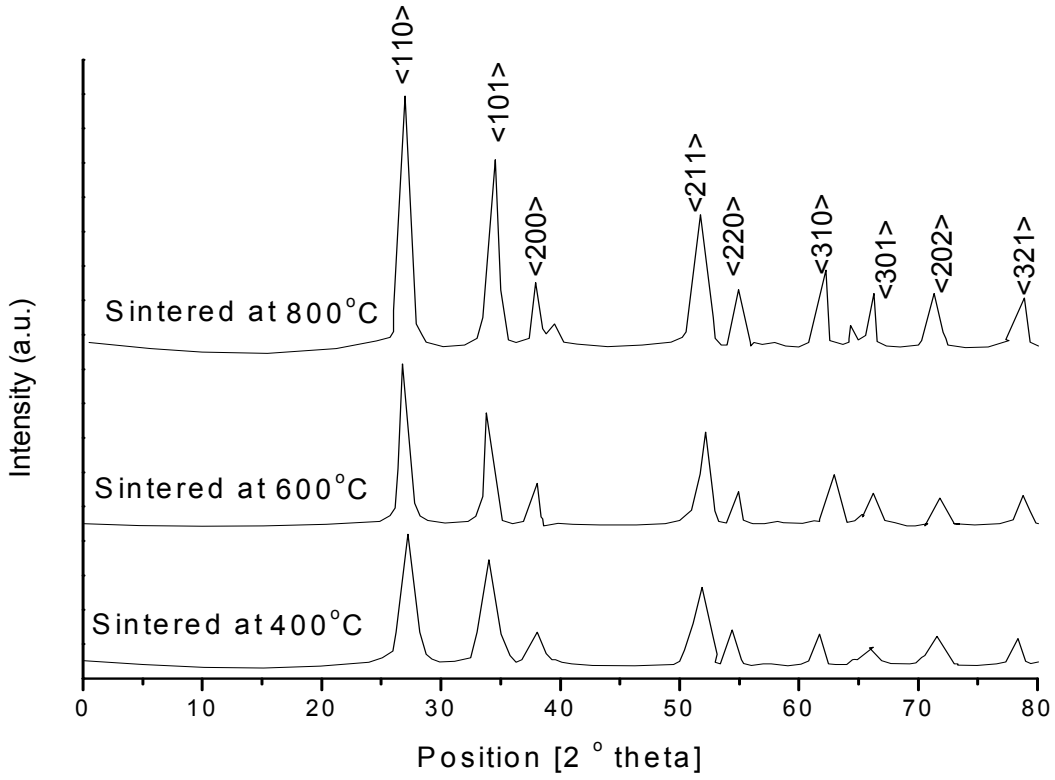

Fig. 7 XRD of SnO_2 powder synthesized at 50°C and sintered at 400, 600 & 800°C

6.4 Effect of Reaction Temperature. The images represented in figures 8-16 are TEM micrographs of SnO_2 synthesized at 5, 25 and 50°C and sintered at 400, 600 and 800°C, respectively. Tin dioxide particles synthesized at 5, 25 and 50°C, followed by sintering at 400°C

yielded particles of average sizes of 2, 10 and 5 nm, respectively. It is evident that particles of SnO_2 synthesized at 5°C and 50°C are smaller than those prepared at 25°C. These results may be explained by the nucleation and growth of particles in a solution. Particle morphology is influenced by the factors such as supersaturation, nucleation and growth rates, colloidal stability, recrystallization and aging process. Generally, supersaturation, which is highly dependent on solution temperature, has a predominant influence on the morphology of the precipitates. A highly supersaturated solution possesses high Gibbs free energy. The tendency of a system to lower its Gibbs free energy is the driving force in the processes of nucleation and growth of particles. The relation between Gibbs free energy change per unit volume, ΔG_v, and supersaturation is given by the following equation:

$$\Delta G_v = - [kT/\Omega] \ln(C/C_0) = - [kT/\Omega] \ln(1+\sigma) \quad (6.4)$$

where C is the concentration of the solute, C_0 is the equilibrium concentration or solubility, k is the Boltzmann constant, T is the temperature, Ω is the atomic volume and σ is the supersaturation defined by $(C- C_0)/C_0$ as reported by Cao [62]. Without supersaturation (i.e. σ), ΔG_v is zero, and no nucleation would occur. It is clear from the relation that ΔG_v can be significantly increased by increasing the supersaturation for a system. Now the supersaturation is temperature as well as rate of reaction dependent. At low temperature (5 °C in present study) a higher supersaturation leads to large reduction in Gibbs free energy. This energy reduction appears as an increased surface energy favouring continued nucleation with smaller sizes. An increased temperature to 25 °C leads to the increased solubility and hence reduced supersaturation of the solution and as a consequence large size particles were obtained. The high temperature (50 °C in present study) favours a fast hydrolysis reaction and results in the high supersaturation, a large ΔG_v, which in turn leads to the formation of a large number of small nuclei [62].

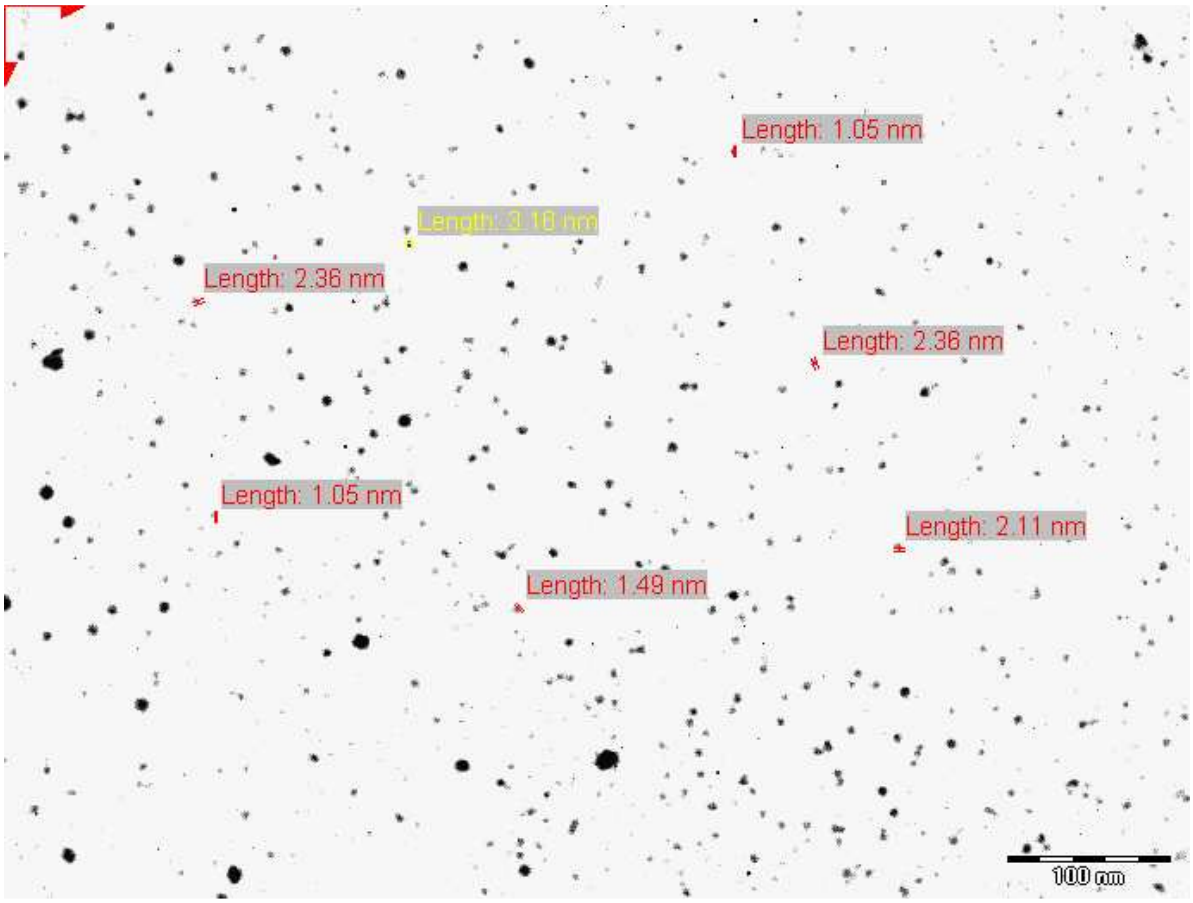

Fig. 8 TEM micrograph of SnO_2 nanoparticles synthesized at 5°C and sintered at 400°C

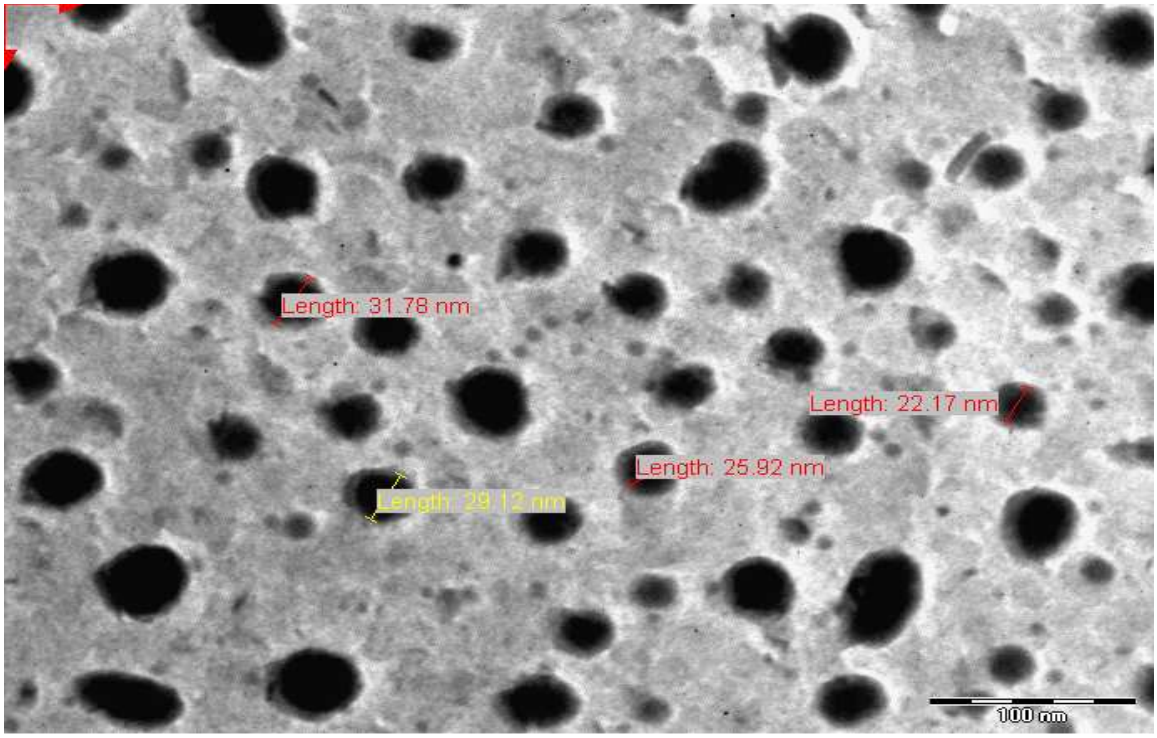

Fig. 9 TEM micrograph of SnO_2 nanoparticles synthesized at 5°C and sintered at 600°C

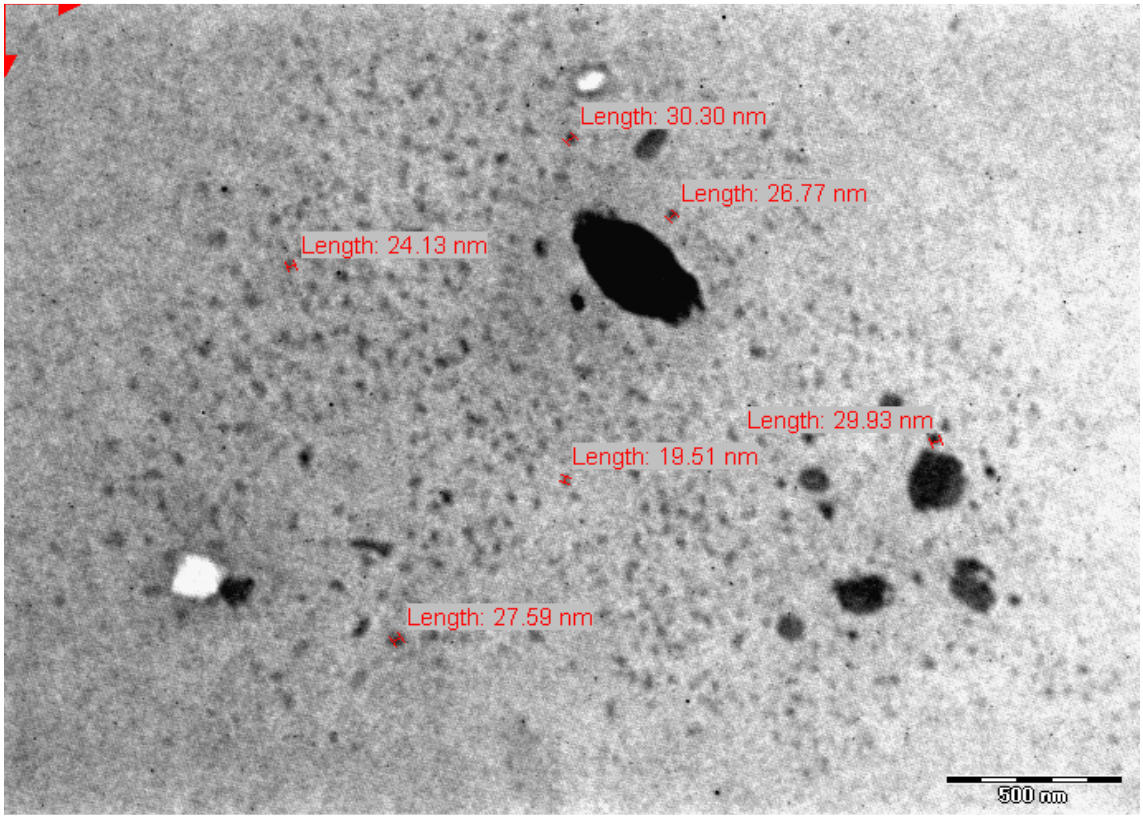

Fig. 10 TEM micrograph of SnO_2 nanoparticles synthesized at 5°C and sintered at 800°C

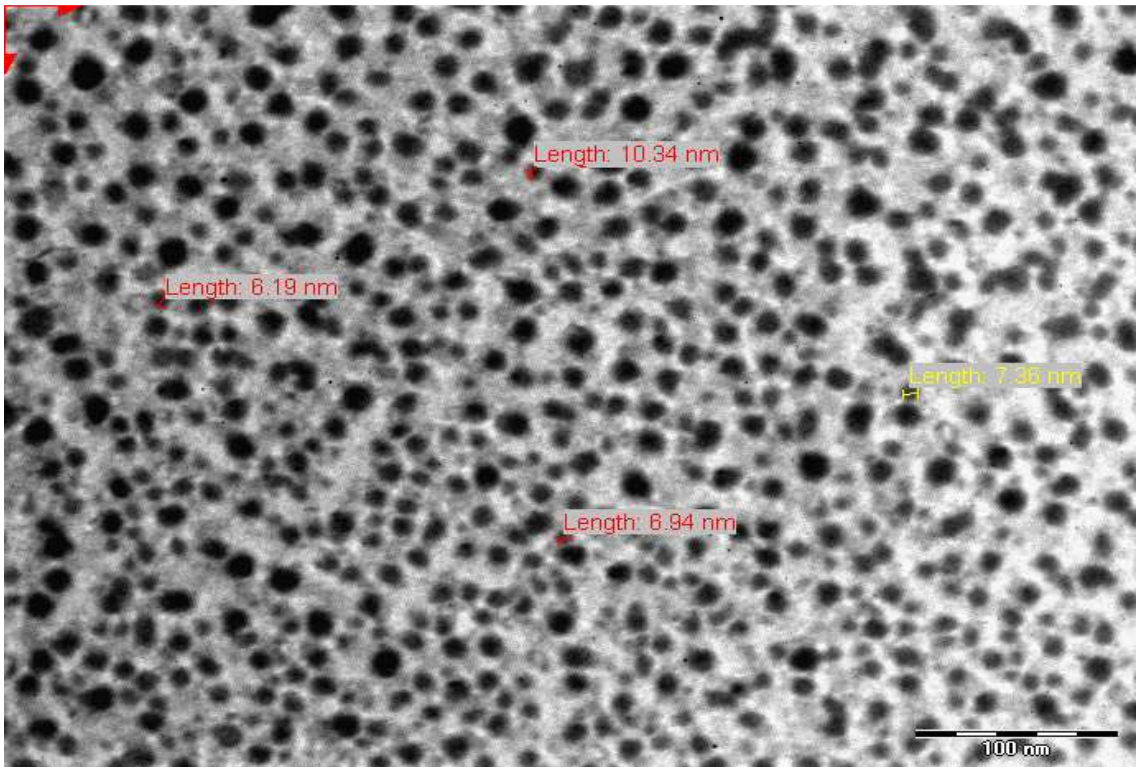

Fig. 11 TEM micrograph of SnO_2 nanoparticles synthesized at 25°C and sintered at 400°C

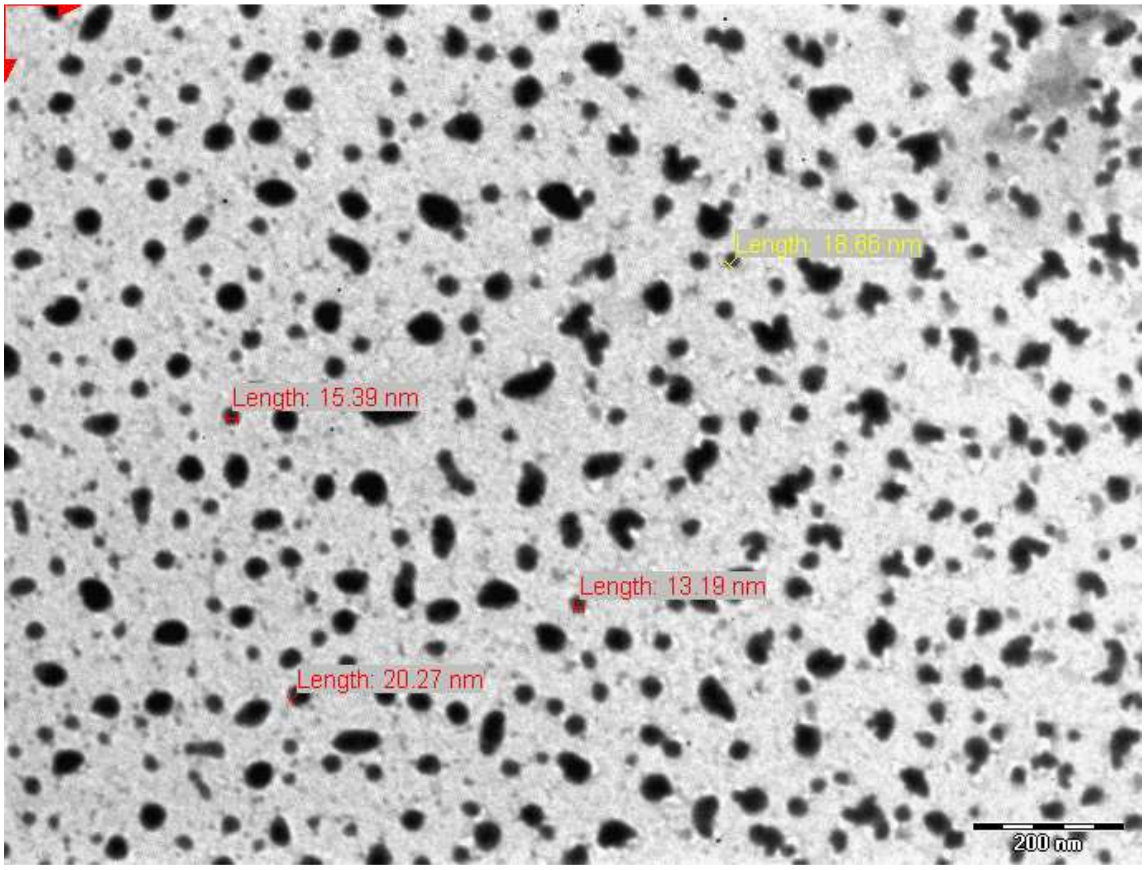

Fig. 12 TEM micrograph of SnO_2 nanoparticles synthesized at 25°C and sintered at 600°C

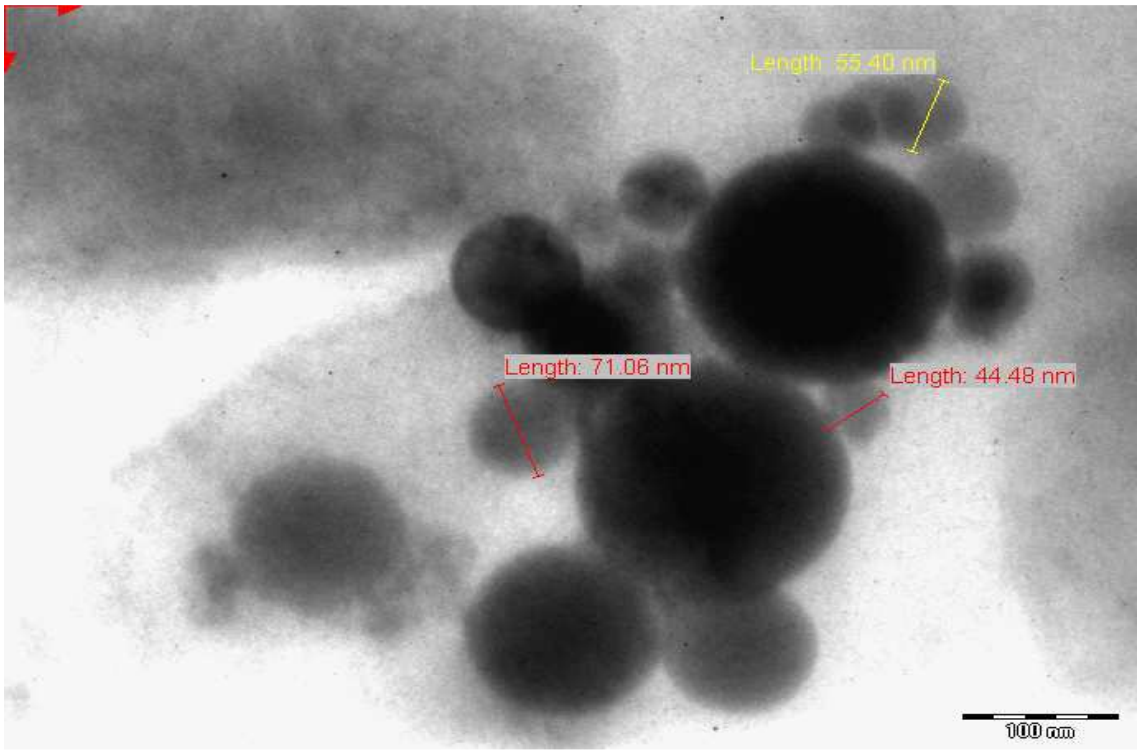

Fig. 13 TEM micrograph of SnO_2 nanoparticles synthesized at 25°C and sintered at 800°C

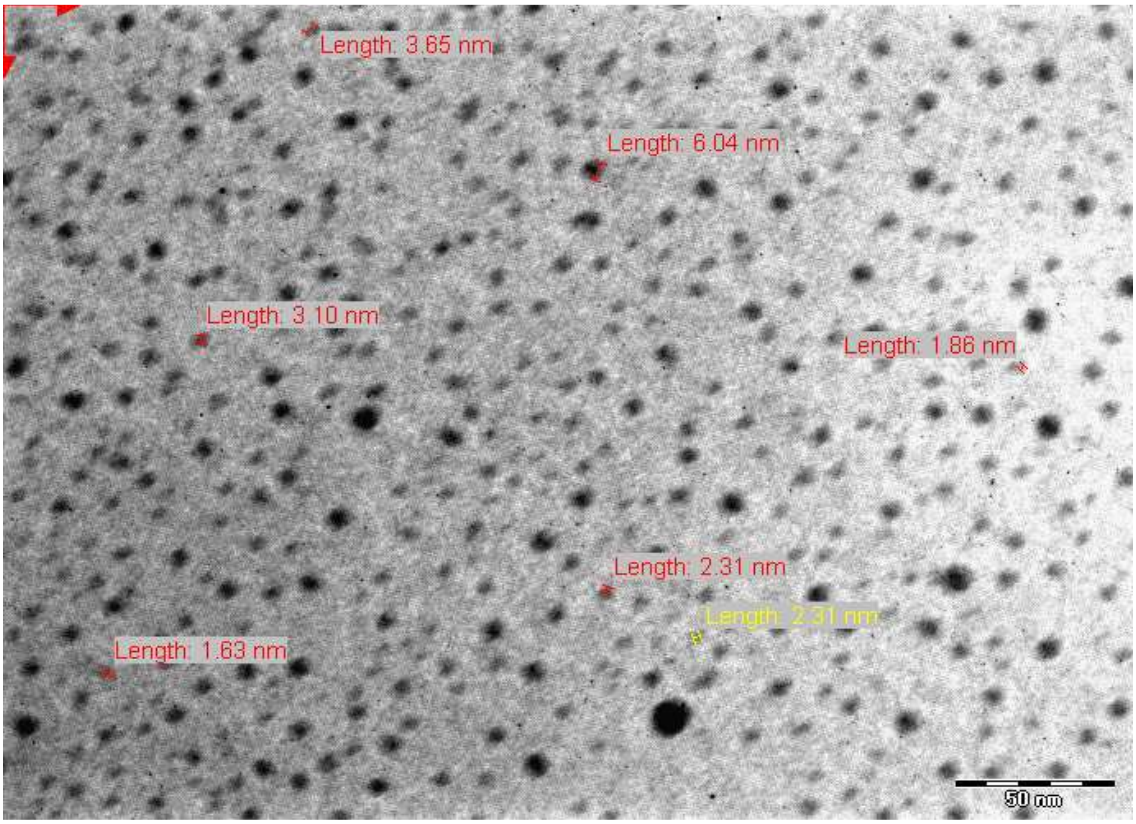

Fig. 14 TEM micrograph of SnO_2 nanoparticles synthesized at 50°C and sintered at 400°C

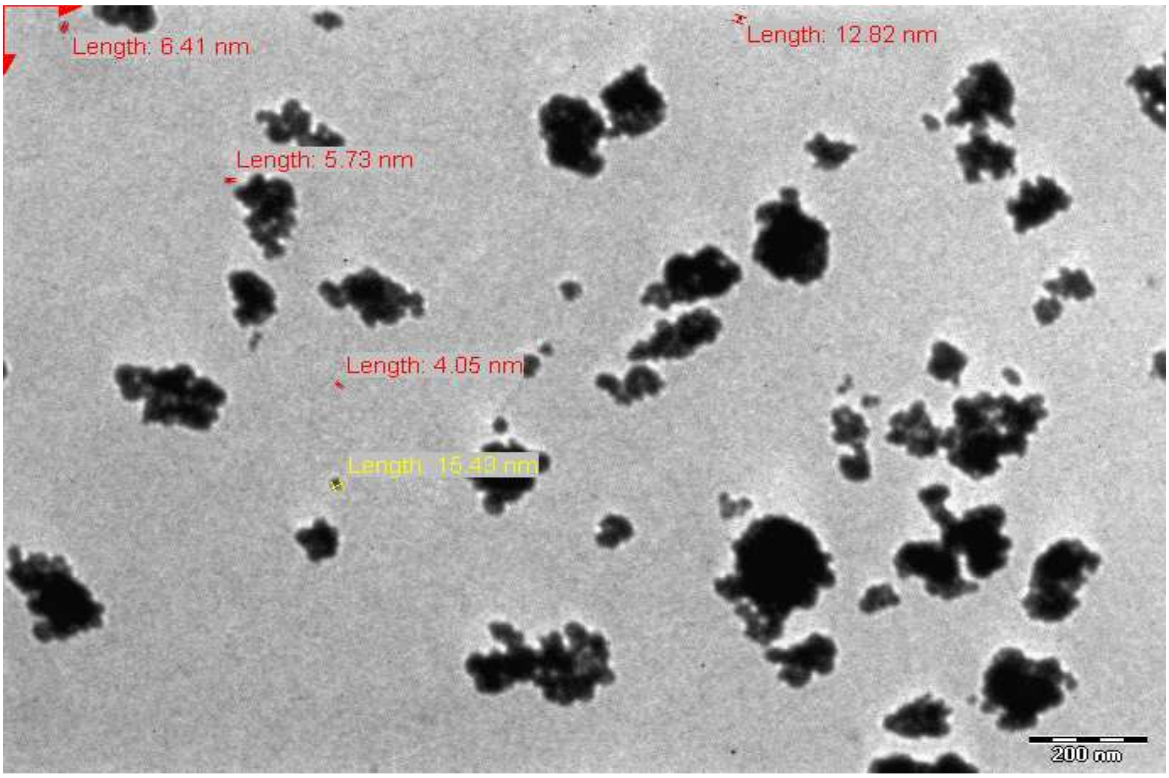

Fig. 15 TEM micrograph of SnO_2 nanoparticles synthesized at 50^oC and sintered at 600^oC

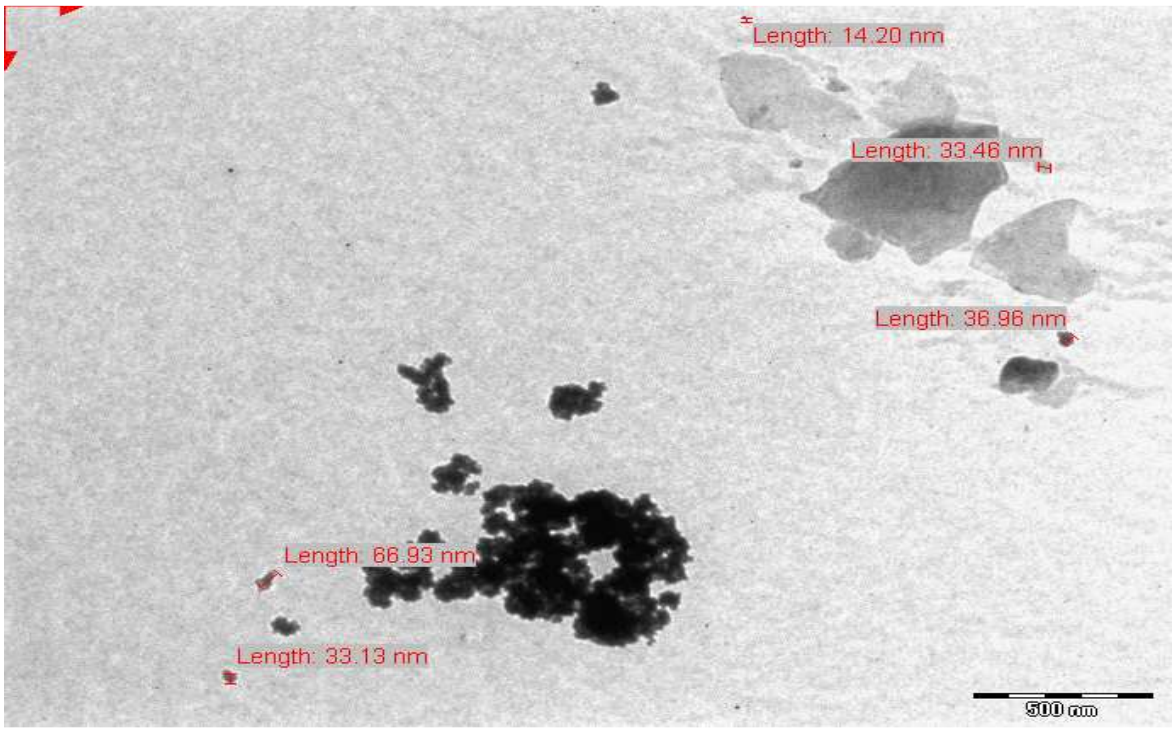

Fig. 16 TEM micrograph of SnO_2 nanoparticles synthesized at 50^oC and sintered at 800^oC

6.5 Effect of Sintering Temperature. The effect of sintering on particle size growth is represented in the TEM micrographs (Figs. 8-16). Some agglomeration along with individual particles is also seen in the micrographs. The average particle sizes observed at different sintering conditions are given in the table 1. Evidently, the sintering temperature promotes enlargement of grain boundaries and consequently, the particle size increases as a function of sintering temperature. Macroscopically, the reduction of total surface energy is the driving force for sintering and

microscopically, the differential surface energy of surfaces with different surface curvature is the true driving force for the mass transport during sintering. Therefore, the results obtained in our study are in accord with the results reported by the other authors [13, 53].

6.6 Sensing Characteristics. Sensors fabricated with synthesized materials were exposed to 200 ppm of ethanol vapours at different temperatures to find out optimum operable temperature which was found for all the samples and is listed in table 1. In general, observations reveal that smaller particles have optimum temperature around 250°C and as particles grow in size and/or agglomerate, the optimum temperature shifts around 350°C.

To study the effect of sintering on the sensing response of the synthesized SnO_2 nanoparticles, the fabricated sensors prepared with materials sintered at temperatures mentioned above were tested with fixed volume of the ethanol vapours at optimum operable temperature. The results of sensor sensitivity versus time for nanoparticles prepared at 5, 25 and 50°C and sintered at 400, 600 and 800°C, respectively, are shown in figure 17. The sensitivity of the samples prepared by sintering at 400°C is exceptionally better than the samples treated at 600 and 800°C, respectively.

Further investigations were carried out with the samples sintered at 400°C. Figure 18 represents sensor sensitivity versus ethanol concentration for sensors prepared at 5, 25 and 50°C, respectively, and sintered at 400°C. The curves show similar trend for all the sensors. Figure 19 shows the comparison of sensitivities of best selected sensors. SnO_2 particles prepared at 5°C and sintered at 400°C are highly sensitive amongst the lot, with the maximum sensitivity of 15. An important point to note is that no catalyst has been incorporated to improve the response of the material. The results were found to be reproducible as fabricated sensors were tested at regular intervals for the period of a year. The comparison between the sensitivity and particle size of SnO_2 at different preparation parameters is given in the table 1. Figure 20 represents the variation of sensitivity versus the particle size of all the nine samples. The sensitivity decreases as the particle size increases.

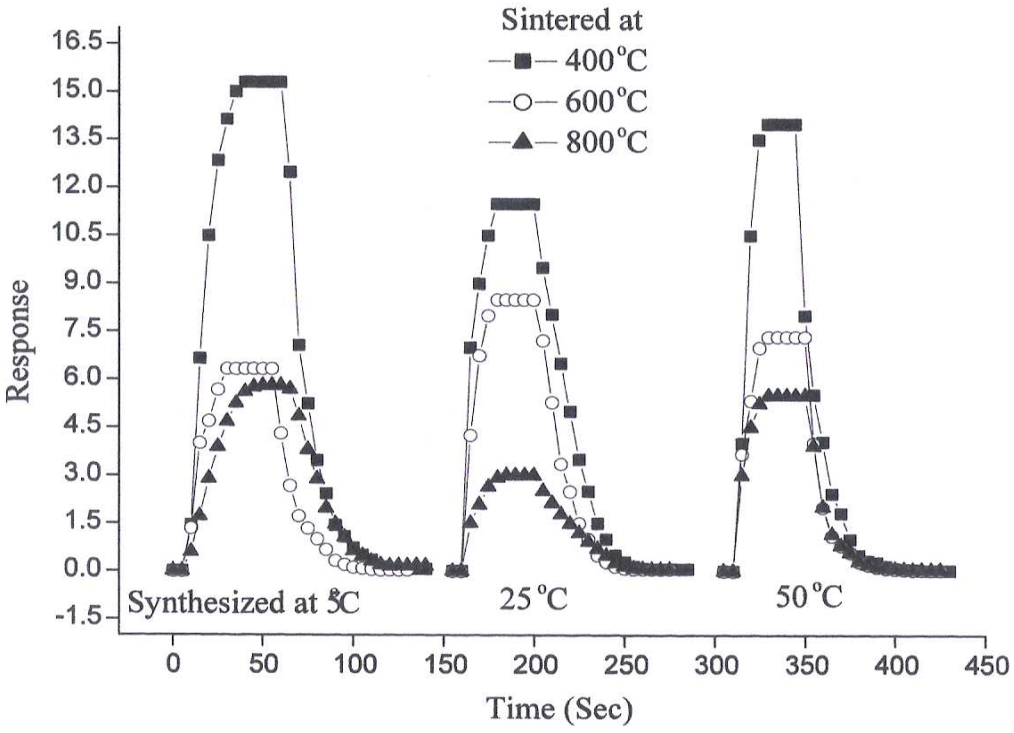

Fig. 17 Comparative sensing response of SnO_2 nanoparticles synthesized at different temperatures to 200 ppm of ethanol

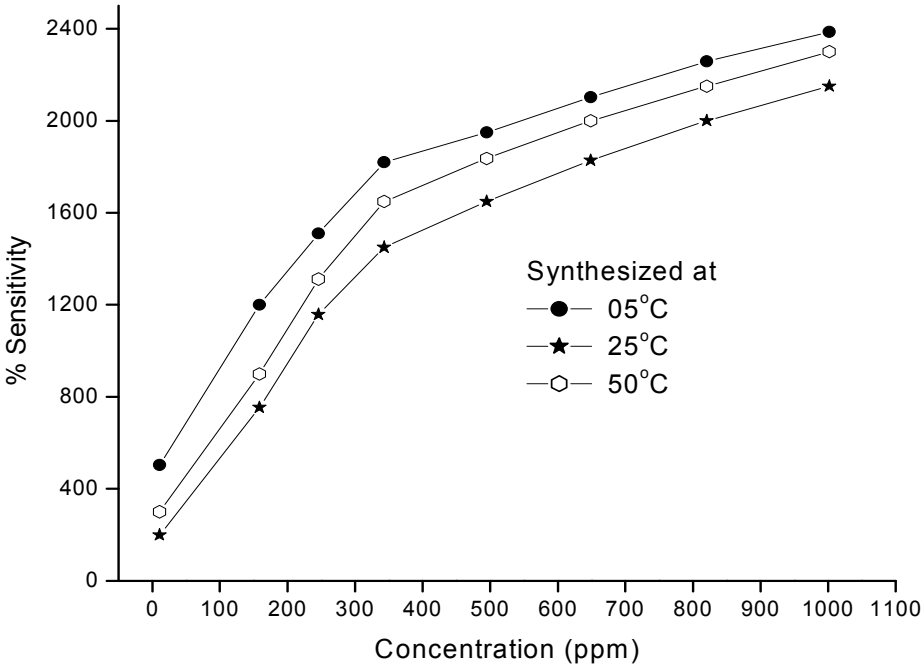

Fig. 18 Sensing response of SnO_2 synthesized at different temperatures and sintered at 400°C as a function of ethanol concentration

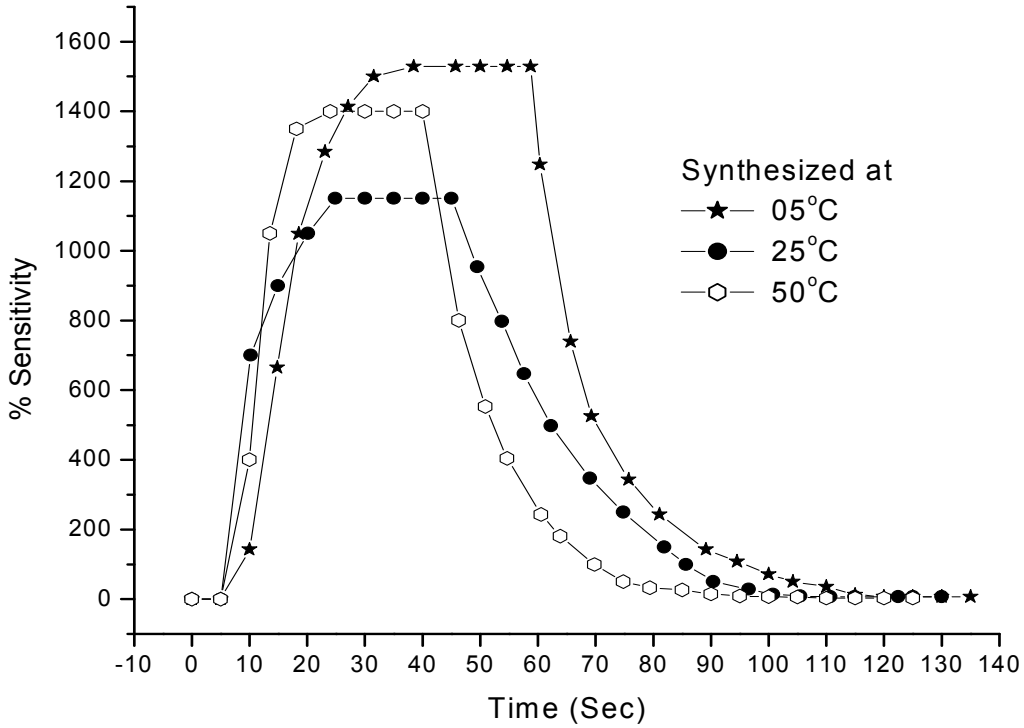

Fig. 19 Comparison of sensing response of SnO_2 synthesized at different temperatures and sintered at 400°C (200 ppm ethanol).

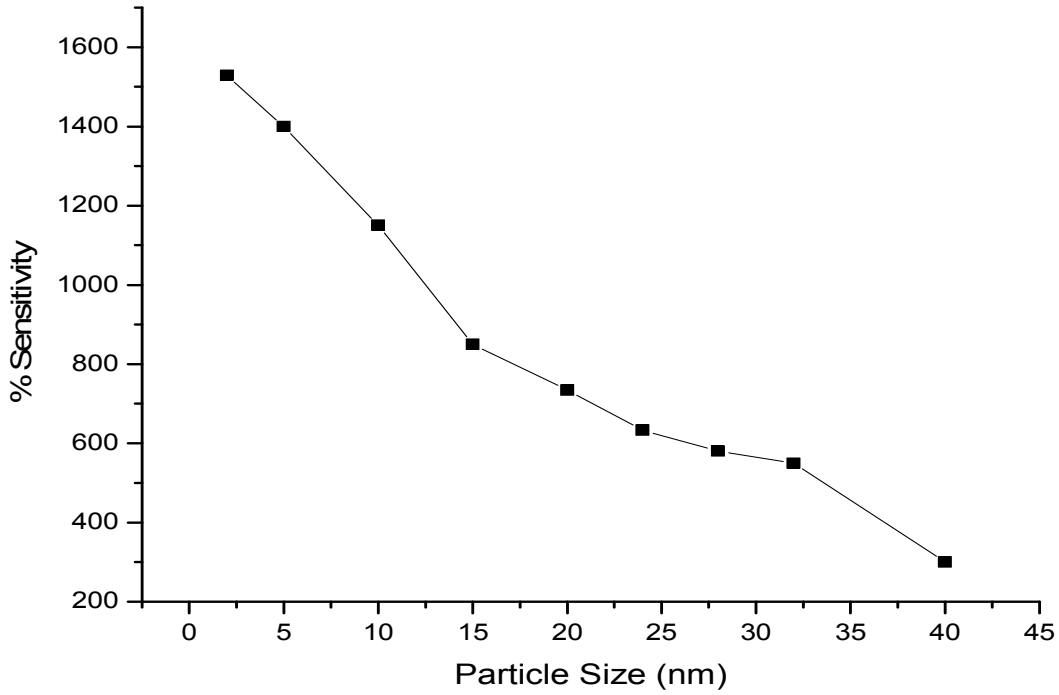

Fig. 20 Sensor response as a function of particle size (200 ppm ethanol)

The gradual decrease in sensing response is because of the growth of particle size with sintering and reaction temperature. A high surface to volume ratio of nanostructures is believed to be one of the important parameters responsible for enhanced sensing response. As the particle size increases with sintering temperature, the surface to volume ratio decreases and consequently sensor response decreases. Nevertheless, nanoparticles of smaller size have larger effective surface area which leads to enhancement in their surface activity. Moreover, a large number of small particles can be accommodated on a unit surface area. These contribute to a large number of particle-particle contacts or active sites onto which gaseous species adsorb to initiate sensing process. Large particles offer less number of such sites because of obvious reasons and consequently are less sensitive.

7. Summary

Nanostructured materials are those with at least one dimension falling in nanometer scale, and include nanoparticles (including quantum dots, when exhibiting quantum effects), nanorods and nanowires, thin films, and bulk materials made of nanoscale building blocks or consisting of nanoscale structures. Many technologies have been explored to fabricate nanostructures and nanomaterials. Proper control of grain size remains a key challenge for high sensor performance. As gas sensing is a complex mechanism and it depends on numerous factors, it is clear that we have to consider the influence of a number of structural parameters of metal oxide matrix on gas sensor response. These parameters are enumerated as thickness, grain size, porosity, grain faceting, agglomeration, film texture, surface geometry, sensor geometry, surface disordering, bulk stoichiometry, grain network, active surface area and size of necks. It has been established that the grain size and the width of the necks are the main parameters that control gas-sensing properties in metal oxide films as well.

Influence of synthesis and sintering temperatures on particle size and ethanol sensing behavior of chemically synthesized tin dioxide (SnO_2) nanostructures has been investigated. SnO_2 particles synthesized at 5, 25 and 50^{o}C, followed by sintering at 400^{o}C, yielded particles of average sizes of

2, 10 and 5 nm, respectively. XRD analysis confirmed that the synthesized SnO_2 nanostructures were of the tetragonal geometry. The results of sensor sensitivity versus time for nanoparticles prepared at 5, 25 and 50^oC and sintered at 400, 600 and 800^oC, respectively, represent some unique features. The sensitivity of the samples prepared by sintering at 400^oC is exceptionally better than the samples treated at 600 and 800^oC, respectively. SnO_2 particles prepared at 5^oC and sintered at 400^oC are highly sensitive amongst the lot, with the maximum sensitivity of 15. It may be noted that no catalyst has been incorporated to improve the gas-sensing response of the SnO_2 material. In general, the sensitivity decreases as the particle size increases. It can be inferred that the optimization of the structural parameters of metal oxides, such as grain size, is an important factor for improving gas sensing characteristics of resistive type sensors.

Acknowledgments

Authors would like to thank the following institutions for providing technical support: CIL Punjab University, Chandigarh for XRD analysis; SAIF, All India Institute of Medical Sciences, New Delhi for TEM investigations.

References

[1] M.J. Madou and S.R. Morrison, Chemical Sensing with Solid State Devices, Academic Press, New York, 1989.

[2] W. Gopel and K.D. Schierbaum, Current status and future prospects, Sens. Actuators B Chem. 26- 27 (1995) 1-12.

[3] G. Eranna, B.C. Joshi, D.P. Runthala and R.P. Gupta, Oxide materials for development of integrated gas sensors-a comprehensive review, Sol. St. Mater. Sci. 29 (2004) 111-188.

[4] G. Korotcenkov, Practical aspects in design of one-electrode semiconductor gas sensors, Sens. Actuators B Chem. 121 (2) (2007) 664-678.

[5] B. Hoffheins, "Solid State, Resistive Gas Sensors," in: R.F. Taylor and J.S. Schultz (Eds.), Handbook of Chemical and Biological Sensors, Philadelphia: Institute of Physics, 1996.

[6] S.A. Hooker, Nanotechnology Advantages Applied to Gas Sensor Development, The Nanoparticles 2002 Conference Proceedings, Business Communications Co., Inc., Norwalk, CT, USA.

[7] W. Gopel, J. Hesse and J.N. Zemel, Sensors: A Comprehensive Survey, Vol. 1-9, Wiley-VCH, Weinheim, 1989-1995.

[8] G. Sberveglieri, Gas Sensors: Principles, Operations and Developments, Kluwer Academic Publishers, Netherlands, 1992.

[9] N. Barsan, M. Schweizer-Belberich and W. Gopel, Fundamental and practical aspects in the design of nanoscaled SnO_2 gas sensor, J. Anal. Chem. 365 (1999) 287-304.

[10] K. Ihokura and J. Watson, Stannic Oxide Gas Sensor: Principle and Applications, CRC Press, Boca Raton, FL, 1994.

[11] K.D. Schierbaum and U. Weimar, Comparison of ceramics, thick-film and thin-film chemical sensors based upon SnO_2, Sens. Actuators B Chem. 7 (1992) 709-716.

[12] D. Kohl, Function and applications of gas sensors, J. Phys. D: Appl. Phys. 34 (2001) R125-R149.

[13] C. Xu, J. Tamaki, N. Miura and N. Yamazoe, Grain size effects on gas sensitivity of porous SnO_2 based elements, Sens. Actuators B Chem. 3 (1991) 147-155.

[14] V. Lantto and T.S. Rantala, Equilibrium and non equilibrium conductance response of sintered SnO_2 samples to CO. Sens. Actuators B Chem. 5 (1991) 103-107.

[15] D.E. Williams and K.F.E Pratt, Classification of reactive sites on the surface of polycrystalline tin dioxide, J. Chem. Soc. Faraday Trans. 94 (1998) 3493-3500.

[16] M.I. Baraton and L. Merhari, Advances in air quality monitoring via nanotechnology, J. Nanoparticle Res. 6 (2004) 107-117.

[17] N. Yamazoe, New approaches for improving semiconductor gas sensors, Sens. Actuators B Chem. 5 (1991) 7-19.

[18] S. Abe, U.-S. Choi, K. Shimanoe and N. Yamazoe, Influences of ball-milling time on gas-properties of Co_3O_4-SnO_2 composites, Sens. Actuators B Chem. 107 (2005) 516-522.

[19] T. Hyoda, N. Nishida, Y. Shimizu and M. Egashira, Preparation and gas-sensing properties of thermally stable mesoporous SnO_2, Sens. Actuators B Chem. 83 (2002) 201-215.

[20] Y. Shimizu, Y. Nakamura and M. Egashira, Effects of diffusivity of hydrogen and oxygen through pores of thick film SnO_2-based sensors on their sensing properties, Sens. Actuators B Chem. 13-14 (1993) 128-131.

[21] T. Hyoda, S. Abe, Y. Shimizu and M. Egashira, Gas-sensing properties of ordered mesoporous SnO_2 and effects of coating there of, Sens. Actuators B Chem. 93 (2003) 590-600.

[22] A. Cabot, A. Dieguez, A. Romano-Rodriguez, J.R. Morante and N. Barsan, Influence of the catalytic introduction procedure on the nano SnO_2 gas sensor performances: Where and how stay the catalytic atoms? Sens. Actuators B Chem. 79 (2001) 98-106.

[23] A. Cirera, A. Cornet, J.R. Morante, S.M. Olaizola, E. Castano and J.R. Gracia, Comparative structural study between sputtered and liquid pyrolysis nanocrystalline SnO_2, Mater. Sci. Eng. B 69-70 (2000) 406-410.

[24] R. Rella, P. Siciliano, S. Capone, M. Epifani, L. Vasanelli and A. Licciulli, Air Quality Monitoring by Means of Sol-Gel Integrated Tin Oxide Thin Films, Sensors and Actuators B 58 (1999) 283- 288.

[25] M. Ferroni, D. Boscarino, E. Comini, D. Gnani, V. Guidi, G. Martinelli, P. Nelli, V. Rigato and G. Sberveglieri, Nanosized Thin Films of Tungsten-Titanium Mixed Oxides as Gas Sensors, Sensors and Actuators B 58 (1999) 289-294.

[26] Y.K. Chung, M.H. Kim, W.S. Um, H.S. Lee, J.K. Song, S.C. Choi, K.M. Yi, M.J. Lee and K.W. Chung, Gas Sensing Properties of WO_3 Thick Film for NO_2 Gas Dependent on Process Conditions, Sensors and Actuators B 60 (1999) 49-56.

[27] A. Chiorino, G. Ghiotti, F. Prinetto, M.C. Carotta, M. Gallana and G. Martinelli, Characterization of Materials for Gas Sensors: Surface Chemistry of SnO_2 and MoO_x-SnO_2 Nano-Sized Powders and Electrical Responses of the Related Thick Films, Sensors and Actuators B 59 (1999) 203-209.

[28] N. Barsan and U. Weimar, Understanding the fundamental principles of metal oxide based gas sensors; the example of CO sensing with SnO_2 sensors in the presence of humidity, J. Phys. Condens. Matter. 15 (2003) R813-R839.

[29] I. Lundstrom, Approaches and mechanisms to solid state based sensing, Sens. Actuators B Chem. 35-36 (1996) 11-19.

[30] N. Barsan and U. Weimar, Conduction model of metal oxide gas sensors, J. Electroceram. 7 (2001) 143-167.

[31] A. Rothschild and Y. Komem, The effect of grain size on the sensitivity of nanocrystalline metal-oxide gas sensors, J. Appl. Phys. 95 (2004) 6374-6380.

[32] K.D. Schierbaum, U. Weimar, W. Gopel and R. Kowalkowski, Conductance, work function and catalytic activity of SnO_2-based gas sensors, Sens. Actuators B Chem. 3 (1991) 205-214.

[33] H. Ogawa, M. Nishikawa and A. Abe, Hall measurements studies and an electrical conduction model of tin oxide ultrafine particle films, J. Appl. Phys. 53 (1982) 4448-4455.

[34] A.C. Bose, P. Thangadurai and S. Ramasamy, Grain size dependent electrical studies on nanocrystalline SnO_2, Mater. Chem. Phys. 95 (2006) 72-78.

[35] B. Timmer, W. Olthuis and A. van den Berg, Ammonia sensors and their applications-a review, Sens. Actuators B Chem. 107 (2005) 666-677.

[36] G. Korotcenkov, Gas response control through structural and chemical modifications of metal oxide films: state of the art and approaches, Sens. Actuators B Chem. 107 (1) (2005) 209-232.

[37] Y. Shimizu and M. Egashira, Basic aspects and challenges of semiconductor gas sensors, MRS Bull. 24 (1999) 18-24.

[38] X. Wang, S.S. Yee and W.P. Carey, Transition between neck-controlled and grain-boundary-controlled sensitivity of metal-oxide gas sensors, Sens. Actuators B Chem. 25 (1995) 454-457.

[39] S.G. Ansari, P. Boroojerdian, S.R. Sainkar, R.N. Karekar, R.C. Aiyer and S.K. Kulkarni, Grain size effects on H_2 gas sensitivity of thick film resistor using SnO_2 nanoparticles, Thin Solid Films 25 (1997) 271-276.

[40] B. Panchapakesan, D.L. De Voe, M.R. Widmaier, R. Cavicchi and S. Semancik, Nanoparticle engineering and control of tin oxide microstructure for chemical microsensor applications, Nanotechnology 12 (2001) 336-349.

[41] M.I. Baraton and L. Merhari, Influence of the particle size on the surface reactivity and gas sensing properties of SnO_2 nanopowders, Mater. Trans. 42 (2001) 1616-1622.

[42] C.N.R. Rao, G.U. Kulkarni, P.J. Thomas and P.P. Edwards, Size-dependent chemistry: Properties of nanocrystals, Chem. Euro. J. 8 (2002) 28-35.

[43] C.H. Shek, J.K.L. Lai and G.M. Lin, Investigation of interface defects in nanocrystalline SnO_2 by positron annihilation, J. Phys. Chem. Sol. 601 (1999) 189-193.

[44] C.V. Thompson, Structure evolution during processing of polycrystalline films, Ann. Rev. Mater. Sci. 30 (2000) 159-190.

[45] A.M. Mazzone, A quantum mechanical study of the stability of SnO_2 nanocrystalline grains, J. Phys.: Cond. Matter 14 (2002) 12819-12824.

[46] N. Goldstein, C.M. Echer and A.P. Alivistos, Melting in semiconductor nanocrystals, Science 256 (1992) 1425-1427.

[47] H.K. Christenson, Confinement effects on freezing and melting, J. Phys. Cond. Matter 13 (2001) 95-133.

[48] Z. Zhang, Z.C. Li and Q. Jiang, Modelling for size-dependent and dimension-dependent melting of nanocrystals, J. Phys. D: Appl. Phys. 33 (2000) 2653-2656.

[49] S.R. Morrison, Semiconductor gas sensors, Sens. Actuators 2 (1982) 329-341.

[50] P.T. Moseley, Solid state gas sensors, Meas. Sci. Technol. 8 (1997) 223-237.

[51] J. Watson, K. Ihokura, G.S.V. Coles, The tin dioxide gas sensor, Meas. Sci. Technol. 4 (1993) 711-719.

[52] G. Zhang, M. Liu, Effect of particle size and dopant on properties of SnO_2- based gas sensors, Sens. Actuators B 69 (2000) 144-152.

[53] M.K. Kennedy, F.E. Kruis, H. Fissan, B.R. Mehta, S. Stappert, G. Dumpich, Tailored nanoparticle films from monosized tin oxide nanocrystals: Particle synthesis, film formation, and size-dependent gas-sensing properties, J. Appl. Phys. 93 (1) (2003) 551-560.

[54] Z. Ying, Q. Wan, Z.T. Song, S.L. Feng, SnO_2 nanowhiskers and their ethanol sensing characteristics, Nanotechnology 15 (2004) 1682-1684.

[55] Y.J. Choi, I.S. Hwang, J.G. Park, K.J. Choi, J.H. Park, J.H. Lee, Novel fabrication of an SnO2 nanowire gas sensor with high sensitivity, Nanotechnology 19 (2008) 095508.

[56] E.T.H. Tan, G.W. Ho, A.S.W Wong, S. Kawi, A.T.S. Wee, Gas sensing properties of tin oxide nanostructures synthesized via a solid-state reaction method, Nanotechnology 19 (2008) 255706.

[57] J. Kaur, R. Kumar, M.C. Bhatnagar, Effect of indium-doped SnO_2 nanoparticles on NO_2 gas sensing properties, Sens. Actuators B 126 (2007) 478-484.

[58] S. Chacko, M.J. Bushiri, V.K. Vaidyan, Photoluminescence studies of spray pyrolytically grown nanostructured tin oxide semiconductor thin films on glass substrates, J. Phys. D: Appl. Phys. 39 (2006) 4540-4543.

[59] S.K. Kang, Y.K. Yang, J. Mu, Solvothermal synthesis of SnO_2 nanoparticles via oxidation of Sn^{2+} ions at water-oil interface, Colloids Surf. A 298 (2007) 280-283.

[60] P.S. Cho, K.W. Kim, J.H. Lee, Improvement of dynamic gas sensing behaviour of SnO_2 acicular particles by microwave calcinations, Sens. Actuators B 123 (2007) 1034-1039.

[61] G. Gaggiotti, A. Galdikas, S. Kaciulis, G. Mattogno, A. Setkus, Surface chemistry of tin oxide based gas sensors, J. Appl. Phys. 76 (8) (1994) 4467-4471.

[62] T. Oyabu, T. Osawa, T. Kurobe, Sensing characteristics of tin oxide thick film gas sensor, J. Appl. Phys. 53 (11) (1982) 7125-7130.

[63] B.K. Miremadi, R.C. Singh, S.R. Morrison, K. Colbow, A highly sensitive and selective hydrogen gas sensor from thick oriented films of MoS_2, Appl. Phys. A 63 (1996) 271-275.

[64] R.C. Singh, O. Singh, M.P. Singh, P.S. Chandi, Synthesis of zinc oxide nanorods and nanoparticles by chemical route and their comparative study as ethanol sensors, Sens. Actuators B 135 (2008) 352-357.

[65] K. Arshak, I. Gaidan, Development of a novel gas sensor based on oxide thick films, Mater. Sci. Eng. B 118 (2005) 44-49.

[66] G. Cao, Nanostructures and Nanomaterials: Synthesis, Properties & Applications, 1st ed., Imperial College Press, London, 2004, p. 76 & 86.

Functional Nanomaterials and their Applications
10.4028/www.scientific.net/SSP.201

Applications of Nanostructured Materials as Gas Sensors
10.4028/www.scientific.net/SSP.201.131